Redox Biology 54 (2022) 102371

Contents lists available at ScienceDirect

Redox Biology

journal homepage: www.elsevier.com/locate/redox

A bioinspired carbon monoxide delivery system prevents acute kidney injury and the progression to chronic kidney disease

Taisei Nagasaki [a,1], Hitoshi Maeda [a,*,1], Kazuaki Taguchi [b], Hiroki Yanagisawa [a], Kento Nishida [a], Kazuki Kobayashi [a], Naoki Wada [a], Isamu Noguchi [a], Ryota Murata [a], Hiromi Sakai [c], Hiroaki Kitagishi [d], Junji Saruwatari [e], Hiroshi Watanabe [a], Masaki Otagiri [f], Toru Maruyama [a,**]

[a] Department of Biopharmaceutics, Graduate School of Pharmaceutical Sciences, Kumamoto University, Kumamoto, Japan
[b] Division of Pharmacodynamics, Faculty of Pharmacy, Keio University, Tokyo, Japan
[c] Department of Chemistry, Nara Medical University, Nara, Japan
[d] Department of Molecular Chemistry and Biochemistry, Faculty of Science and Engineering, Doshisha University, Kyoto, Japan
[e] Division of Pharmacology and Therapeutics, Graduate School of Pharmaceutical Sciences, Kumamoto University, Kumamoto, Japan
[f] Faculty of Pharmaceutical Sciences and DDS Research Institute, Sojo University, Kumamoto, Japan

ARTICLE INFO

Keywords:
Tubular cell damage
Carbon monoxide
Red blood cells
Acute kidney injury
Acute kidney injury to chronic kidney disease transition

ABSTRACT

Renal ischemia-reperfusion (IR)-induced tissue hypoxia causes impaired energy metabolism and oxidative stress. These conditions lead to tubular cell damage, which is a cause of acute kidney injury (AKI) and AKI to chronic kidney disease (CKD). Three key molecules, *i.e.*, hypoxia-inducible factor-1α (HIF-1α), AMP-activated protein kinase (AMPK), and nuclear factor E2-related factor 2 (Nrf2), have the potential to protect tubular cells from these disorders. Although carbon monoxide (CO) can comprehensively induce these three molecules via the action of mitochondrial reactive oxygen species (mtROS), the issue of whether CO induces these molecules in tubular cells remains unclear. Herein, we report that CO-enriched red blood cells (CO-RBC) cell therapy, the inspiration for which is the *in vivo* CO delivery system, exerts a renoprotective effect on hypoxia-induced tubular cell damage via the upregulation of the above molecules. Experiments using a mitochondria-specific antioxidant provide evidence to show that CO-driven mtROS partially contributes to the upregulation of the aforementioned molecules in tubular cells. CO-RBC ameliorates the pathological conditions of IR-induced AKI model mice via activation of these molecules. CO-RBC also prevents renal fibrosis via the suppression of epithelial mesenchymal transition and transforming growth factor-β1 secretion in an IR-induced AKI to CKD model mice. In conclusion, our results confirm that the bioinspired CO delivery system prevents the pathological conditions of both AKI and AKI to CKD via the amelioration of hypoxia inducible tubular cell damage, thereby making it an effective cell therapy for treating the progression to CKD.

Abbreviations: IR, ischemia-reperfusion; CO, carbon monoxide; Hb, hemoglobin; RBC, red blood cells; CO-RBC, CO-enriched red blood cells; CORM-2, carbon monoxide releasing molecule-2; AKI, acute kidney injury; CKD, chronic kidney disease; AKI to CKD, acute kidney injury to chronic kidney disease transition; ESRD, end-stage renal disease; mtROS, mitochondrial reactive oxygen species; HIF-1α, hypoxia-inducible factor-1α; AMPK, AMP-activated protein kinase; Nrf2, nuclear factor E2-related factor 2; EMT, epithelial mesenchymal transition; TGF-β1, transforming growth factor-β1; HO-1, heme oxygenase-1; VEGF, vascular growth factor; ATP, adenosine triphosphate; NOX, NADPH oxidase; Kim-1, kidney injury molecule-1; COL1A1, Collagen 1A1; PPARγ, peroxisome growth factor-activating receptor γ.

* Corresponding author. Department of Biopharmaceutics, Graduate School of Pharmaceutical Sciences, Kumamoto University, 5-1, Oe-honmachi, Kumamoto, 862-0973, Japan.

** Corresponding author. Department of Biopharmaceutics, Graduate School of Pharmaceutical Sciences, Kumamoto University, 5-1, Oe-honmachi, Kumamoto, 862-0973, Japan.

E-mail addresses: 191y3003@st.kumamoto-u.ac.jp (T. Nagasaki), maeda-h@kumamoto-u.ac.jp (H. Maeda), taguchi-kz@pha.keio.ac.jp (K. Taguchi), yanagisawa.hiroki@kao.com (H. Yanagisawa), 214y3001@st.kumamoto-u.ac.jp (K. Nishida), 217y2002@st.kumamoto-u.ac.jp (K. Kobayashi), 222y2006@st.kumamoto-u.ac.jp (N. Wada), 220y3005@st.kumamoto-u.ac.jp (I. Noguchi), ryota.080708@gmail.com (R. Murata), hirosakai@naramed-u.ac.jp (H. Sakai), hkitagis@mail.doshisha.ac.jp (H. Kitagishi), junsaru@gpo.kumamoto-u.ac.jp (J. Saruwatari), hnabe@kumamoto-u.ac.jp (H. Watanabe), otagirim@ph.sojo-u.ac.jp (M. Otagiri), tomaru@gpo.kumamoto-u.ac.jp (T. Maruyama).

[1] These authors contributed equally: Taisei Nagasaki, Hitoshi Maeda.

https://doi.org/10.1016/j.redox.2022.102371
Received 25 April 2022; Received in revised form 13 June 2022; Accepted 13 June 2022
Available online 22 June 2022

1. Introduction

Chronic kidney disease (CKD) is a high-risk disease that eventually leads to end-stage renal disease (ESRD) and is characterized by interstitial fibrosis [1,2]. Its prevalence is about 10% worldwide, and the number of patients continues to increase year by year [3]. Unfortunately, the lost renal function of CKD patients cannot be recovered, and there is currently no reliable treatment for both CKD and ESRD. Given this fact, the development of a new therapeutic strategy for preventing the progression to CKD would be highly desirable.

Acute kidney injury (AKI) is a disease in which renal function declines rapidly with a transient loss of tubular cells [4]. There is a positive correlation between the severity or frequency of AKI and the degree of renal fibrosis [5,6]. A recent epidemiological study reported that 25% of AKI patients, who recovered their renal function, eventually progress to CKD [7]. Thus, AKI is recognized as an independent risk factor for CKD [8]. During the progression to CKD from AKI, an abnormal condition develops in which incompletely repaired tubular cells remain in the kidney [9]. Ishani, A. et al. defined this condition as an AKI to CKD transition (AKI to CKD), which is a new concept in renal pathology [10]. Therefore, new therapeutic strategies that can alleviate the tubular cell damage common to AKI and AKI to CKD have the potential to inhibit the progression to CKD.

Ischemia-reperfusion (IR), which is carried out during renal transplantation and cardiovascular surgery, causes tissue hypoxia [11]. The condition induces impaired energy metabolism [12] and oxidative stress [13], leading to tubular cell apoptosis. Mildly damaged tubular cells can be completely repaired through the process of dedifferentiation and proliferation, whereas severe damage results in incomplete repair due to the reduced level of adenosine triphosphate (ATP) production which is required for tissue repair [14]. These incomplete cells are transformed into fibroblasts via an epithelial mesenchymal transition (EMT) and subsequently activate surrounding fibroblasts via the secretion of humoral factors such as transforming growth factor-β1 (TGF-β1), resulting in the development of renal fibrosis [9].

As of this writing, it has been reported that the activation of the following three molecules suppresses tubular cell damage due to the pharmacological benefit; 1) hypoxia-inducible factor-1α (HIF-1α) to improve tissue hypoxia [15], 2) AMP-activated protein kinase (AMPK) to maintain intracellular energy homeostasis [16] and 3) nuclear factor E2-related factor 2 (Nrf2) to control the antioxidant mechanisms [17]. Moreover, a dual agonist of Nrf2 and AMPK synergistically enhances their effects compared to each single agonist [18]. Therefore, bioactive substances, which can comprehensively activate these three molecules, would be expected to ameliorate tubular cell damage.

Carbon monoxide (CO) is widely recognized as toxic gas, high concentrations of which can cause rapid death due to respiratory depression [19,20]. However, recent advances in gas biology have revealed that low concentrations of CO are constantly produced inside the body by the action of heme oxygenase-1 (HO-1), and the resulting CO functions as an intracellular signal transduction molecule [21–24]. Interestingly, CO promotes HIF-1α stabilization [25–27], the phosphorylation of AMPK [26,28–30] and the nuclear translocation of Nrf2 [31,32] in various cells. These findings led us to hypothesize that CO might have the potential to improve the pathological conditions of both AKI and AKI to CKD through the activation of these signaling pathways. However, there is currently no information available on whether CO influences the HIF-1α, AMPK and Nrf2 pathways in tubular cells, thereby exhibiting renoprotective effects on AKI or AKI to CKD.

The CO that is inhaled is then delivered to the blood via the lung. Most of the CO binds to a part of hemoglobin (Hb) in red blood cells (RBC) and then circulates in the blood [33,34]. The resulting CO is then supplied to organs [35]. In other words, this represents an *in vivo* CO delivery system. To apply CO *in vivo*, we previously established a cell therapy using CO-enriched RBC (CO-RBC) in which instead of oxygen (O_2), CO is bound to almost all the Hb molecules of RBC [36–38]. This bioinspired CO delivery system was found to improve the lethality of rats with massive hemorrhagic shock in a manner that was equivalent to O_2 bound RBC (O_2-RBC) because CO-RBC functions as a dual gas donor of both CO and O_2[39].

The aim of this study was to clarify the cytoprotective effect of CO on tubular cells, and subsequently, the renoprotective effect of CO-RBC on two types of experimental model mice, *i.e.*, an IR-induced AKI model (IR-AKI) and an IR-induced AKI to CKD model (IR-AKI to CKD).

2. Results

2.1. CO activates HIF-1α, AMPK and Nrf2 in HK-2 cells

We first investigated the activation of HIF-1α, AMPK and Nrf2 after treating HK-2 cells, a type of human proximal tubular cell, with O_2-RBC or CO-RBC (1.0×10^7 cells/ml) for 0, 1, 3 and 6 h. Surprisingly, no obvious differences were found for the induction of HIF-1α, the phosphorylation of AMPK and the nuclear translocation of Nrf2 between the two treatments (S. Fig. 1A and B). This finding was also confirmed by the protein levels of the vascular growth factor (VEGF) and HO-1, both of which are downstream proteins that are regulated by HIF-1α and Nrf2, respectively (S. Fig. 1A). Considering the fact that human tubular cells are exposed to abundant RBC in the blood, these results suggest that endogenous proteins derived from RBC, such as Hb [40], have an impact on the levels of the above proteins.

To examine the effect of CO-RBC under physiological conditions, we preconditioned HK-2 cells with O_2-RBC. The protein levels of HIF-1α and the phosphorylation of AMPK increased transiently for periods of up to 48 h after the O_2-RBC preconditioning, and the levels then decreased to those of the controls (S. Fig. 1A and C). In addition, the nuclear translocation of Nrf2 was not increased at 96 h after the O_2-RBC preconditioning (S. Fig. 1D). These led us to conclude that HK-2 cells that had been pre-treated with O_2-RBC for 96 h acquired the characteristics of human tubular cells. After treating the preconditioned HK-2 cells with CO-RBC for 6 h, the protein levels of HIF-1α, the phosphorylation of AMPK, and the nuclear translocation of Nrf2 were increased, while these effects were not observed in the case of the O_2-RBC treatment (S. Fig. 1E and F).

As discussed above, *in vitro* experiments using RBC are complicated and time-consuming. Because of this, we used CORM-2 as a CO donor [41] in the subsequent experiments to determine the effect of CO on tubular cells. Consistent with the results obtained for the CO-RBC treatment shown in S. Fig. 1E and F, the treatment with 100 μM CORM-2 resulted in the upregulation of the protein levels of HIF-1α and the phosphorylation of AMPK, as well as the nuclear translocation of Nrf2 (Fig. 1A and B). These phenomena were also confirmed by the protein levels of VEGF and HO-1 (Fig. 1A). On the other hand, these effects were not observed in the case of the treatment with inactive CORM-2 (iCORM-2) (S. Fig. 2A and B). In addition, the 100 μM CORM-2 treatment had no effect on the viability of HK-2 cells (S. Fig. 2C). These findings led us to conclude that the CO derived from CORM-2 contributes to the activation of the above proteins.

CO-driven mitochondrial reactive oxygen species (mtROS) are attributed to activate HIF-1α, AMPK and Nrf2 [25,28,31]. Therefore, we co-treated HK-2 cells with CORM-2 and Mito-TEMPO (10 μM), a mitochondria-specific antioxidant [42], to confirm whether Mito-TEMPO attenuates the CO-induced protein levels of each molecule or the nuclear translocation of Nrf2. The CORM-2-induced protein levels of HIF-1α and VEGF was suppressed with the treatment of Mito-TEMPO, whereas such phenomena were not observed for the protein levels of phosphorylation of AMPK and HO-1 or the nuclear translocation of Nrf2 (Fig. 1C–E).

2.2. CO activates HIF-1α, AMPK and Nrf2 in HK-2 cells under hypoxia condition

Considering the pathological conditions of the kidney, we assessed the issue of whether CO under hypoxia condition activates HIF-1α, AMPK and Nrf2. HK-2 cells were treated with CORM-2 in an experimental hypoxia chamber for 48 h. The development of hypoxia resulted in an increase in the protein levels of HIF-1α and the phosphorylation of AMPK, but did not alter VEGF protein levels. On the other hand, treatment with CORM-2 under hypoxia condition resulted in a great

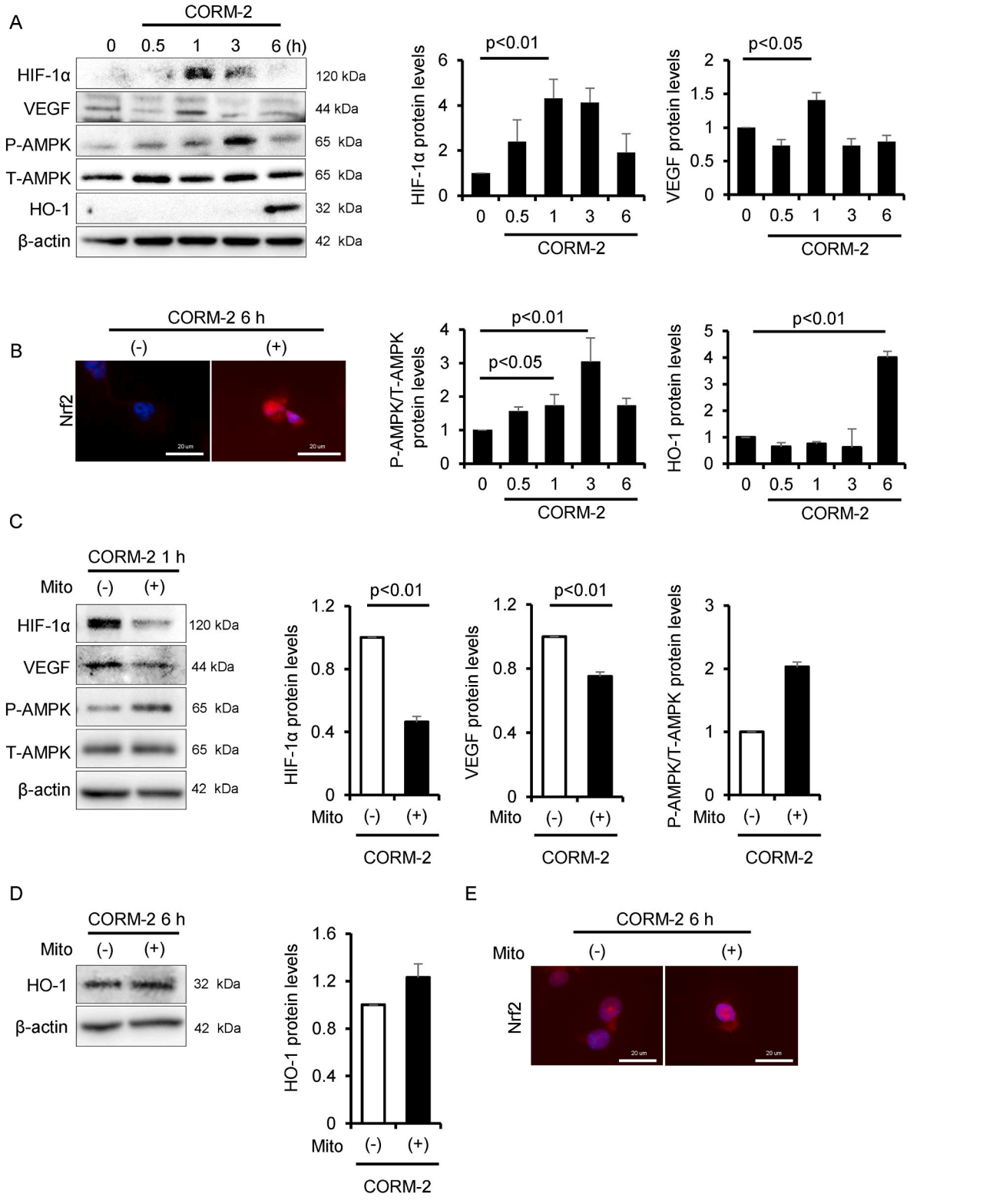

Fig. 1. CO activates HIF-1α, AMPK and Nrf2. To evaluate the effect of CO on the activation of HIF-1α, AMPK and Nrf2, HK-2 cells were treated with CORM-2 (100 μM) for 0, 0.5, 1, 3 and 6 h, then analyzed by (A) immunoblot (n = 3/group) and (B) immunofluorescence. To confirm CO-driven mtROS on the activation of these molecules, HK-2 cells were treated with Mito-TEMPO (Mito, 10 μM) for 30 min before CORM-2 treatment, then analyzed by (C, D) immunoblot (n = 3/group) and (E) immunofluorescence. Results are expressed as the mean ± S.E.M.

upregulation in the protein levels of these molecules compared with under this condition alone (Fig. 2A). Further, the nuclear translocation of Nrf2 and HO-1 protein levels 6 h after exposure to hypoxia were increased by the CORM-2 treatment (Fig. 2B and C).

2.3. CO mitigates hypoxia-induced tubular cell damage

We next examined whether CO mitigates hypoxia-induced tubular cytotoxicity. The gene expression of the kidney injury molecule-1 (Kim-1), a marker for tubular cytotoxicity [43], was upregulated under hypoxia condition, but the increase was significantly suppressed by CORM-2 treatment (Fig. 3A). To determine the protective effect of CO derived from CORM-2 against tubular cell damage, we used hemoCD [44] (10 μM), which is a complex of a cyclodextrin and iron porphyrin, in this experiment because it functions as a CO scavenger by coordinating CO to the iron porphyrin contained in this complex. As shown in Fig. 3A, the suppressive effect of CORM-2 on the gene expression of Kim-1 were canceled by the co-treatment with CORM-2 and hemoCD. This finding shows that hemoCD inhibited the intracellular translocation of CO derived from CORM-2 and possibly suppressed the activation of HIF-1α, AMPK and Nrf2, which resulted in the loss of the CO-induced cytoprotective effect. Further, the decreased cell viability under hypoxia condition was restored by the CORM-2 treatment (Fig. 3B). Since intracellular ATP is mainly produced by oxidative phosphorylation with oxygen as a substrate, the levels of ATP were decreased under hypoxia condition, resulting in tubular cell damage [45]. Activated AMPK promotes ATP production via mitochondrial oxidative phosphorylation [46]. Hence, we investigated the issue of whether CO enhances ATP production under hypoxia condition. The decreased ATP levels were restored by the CORM-2 treatment (Fig. 3C). One of the antioxidant capacities of CO is the inhibition of the protein levels of NADPH oxidase (NOX) [47]. Therefore, we evaluated NOX4, which is expressed at the highest level among the NOX isoforms in the kidney [48]. Increased NOX4 protein levels under hypoxia condition were decreased by the CORM-2 treatment (Fig. 3D), and this phenomenon was corroborated by the intracellular ROS levels (Fig. 3E).

2.4. CO inhibits hypoxia-induced EMT

We also examined whether CO exerts an antifibrotic effect on hypoxia-induced EMT. After exposing HK-2 cells to hypoxia for 96 h, the protein levels of α-SMA, a marker for activated fibroblasts [49], and TGF-β1 were increased while the protein levels of E-Cadherin, a marker for tubular epithelial cells [50], was decreased. In contrast, the treatment of CORM-2 under hypoxia condition reversed their expression patterns (Fig. 3F). We next treated NRK-49F cells, rat renal fibroblasts, with the culture supernatant from HK-2 cells which had been treated with the presence or absence of CORM-2 under hypoxia condition. The protein levels of Collagen 1A1 (COL1A1) and α-SMA, both of which indicate the activation of fibroblasts [51], was significantly decreased in the culture supernatant from the HK-2 cells that had been treated with CORM-2 under hypoxia condition (Fig. 3G).

2.5. Pre-administration of CO-RBC improves renal pathology in IR-AKI

To apply CO-RBC *in vivo*, we first measured CO concentration in blood by gas chromatography after a single administration of CO-RBC (1400 mgHb/kg, iv). The concentration of CO in blood transiently increased and then gradually decreased to near the baseline value within 90 min (Fig. 4A), suggesting that CO was distributed to the kidney with 90 min after the administration of CO-RBC. We then measured the amount of CO in the kidney 90 min after the administration of CO-RBC. The CO-RBC administration increased the amount of CO by about 2-fold compared with that of the saline administration group (Fig. 4B).

We prepared IR-AKI mice induced by renal IR, which is the most common cause of AKI [52,53]. Based on the result in Fig. 4B, the

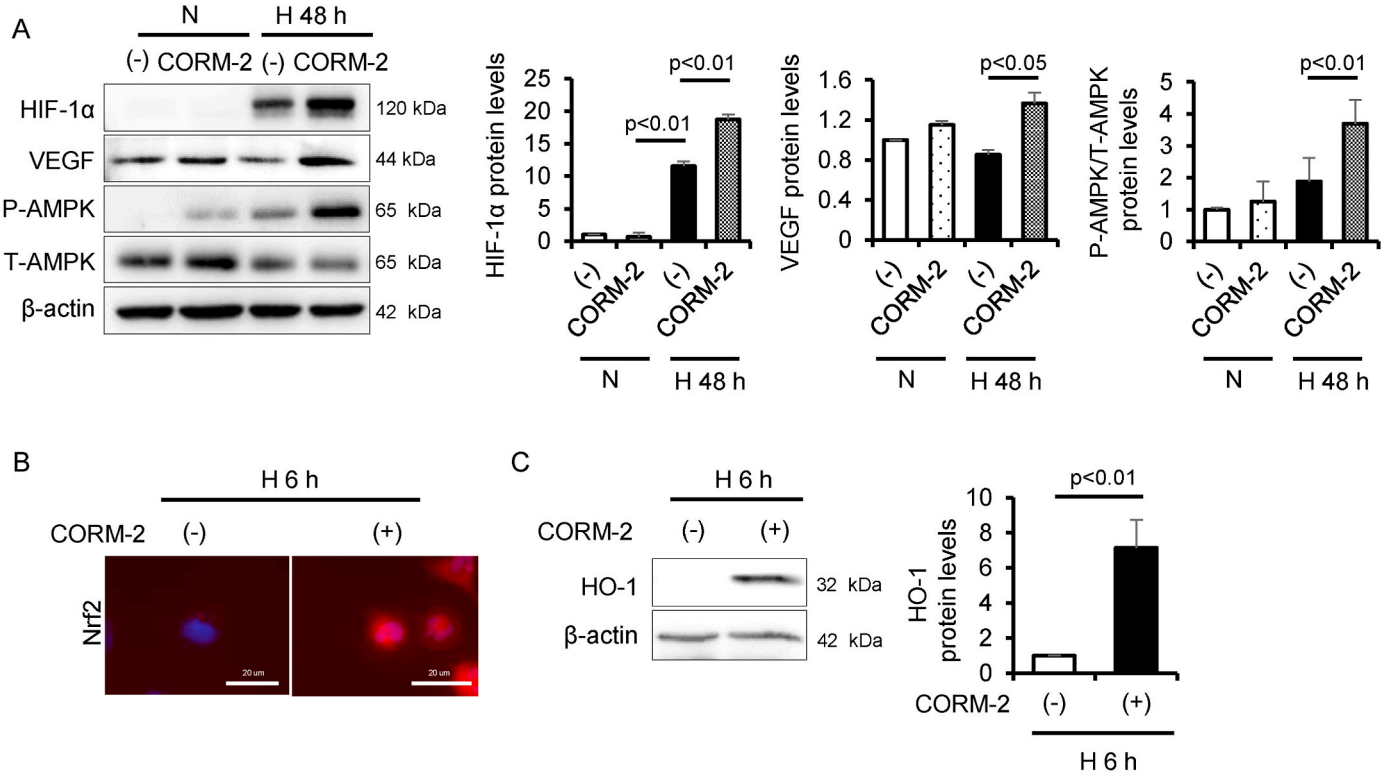

Fig. 2. CO activates HIF-1α, AMPK and Nrf2 under hypoxia condition. To examine the effect of CO on the activation of HIF-1α, AMPK, and Nrf2 under normoxia (N, 21% O_2) or hypoxia condition (H, 0.1% O_2), HK-2 cells were treated with CORM-2 under hypoxia condition for 6 or 48 h, then analyzed by (A, C) immunoblot (n = 3/group) and (B) immunofluorescence. Results are expressed as the mean ± S.E.M.

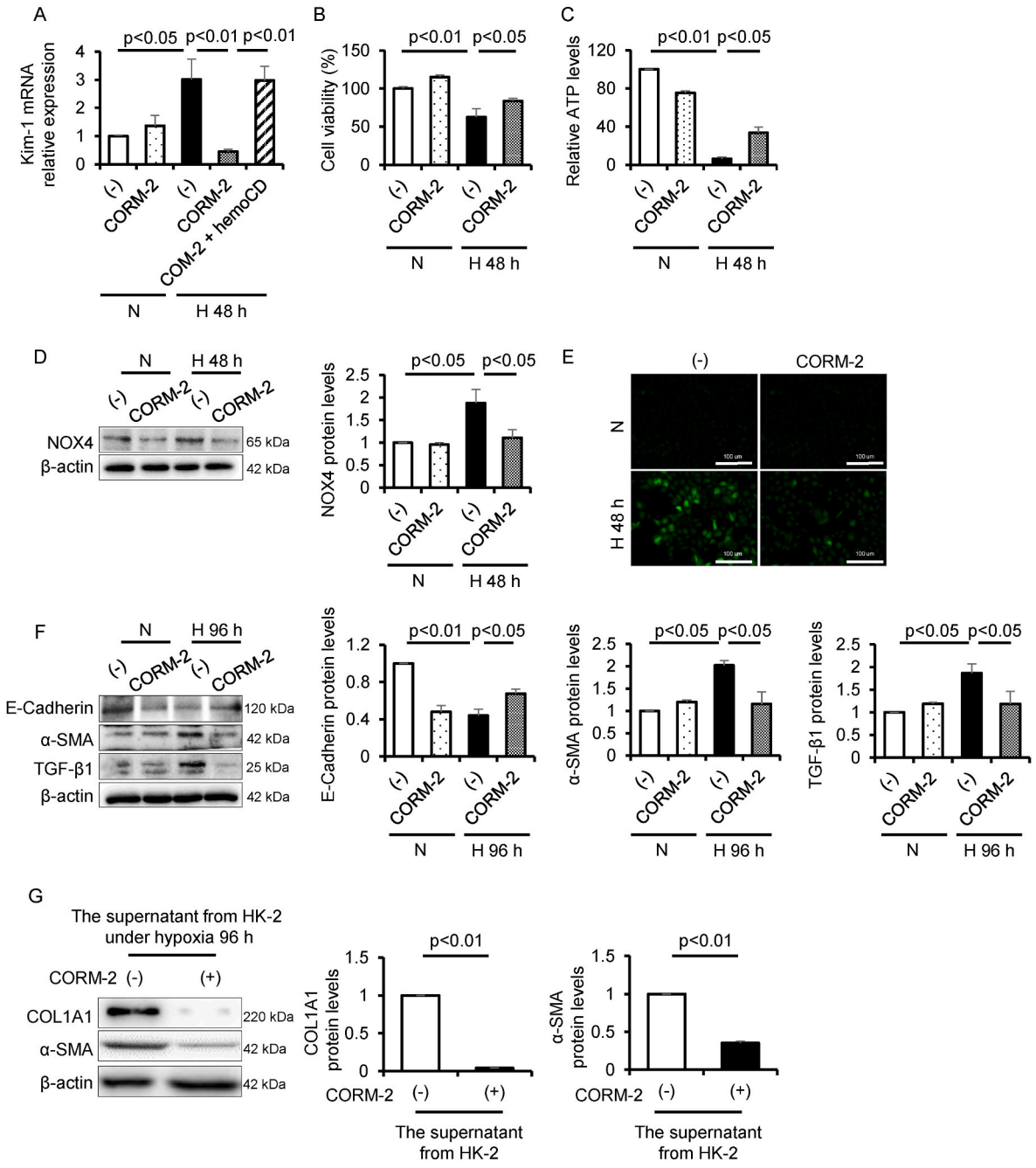

Fig. 3. CO mitigates hypoxia-inducible tubular cell damage. To examine the cytoprotective effect of CO on the tubular cell damage, cell viability, ATP levels, oxidative stress and EMT pathway under hypoxia condition, HK-2 cells were treated with CORM-2 under hypoxia condition for 48 or 96 h, then analyzed by (A) qRT-PCR (n = 3/group), (B) CCK-8 assay (n = 5/group), (C) ATP assay (n = 4/group), (D, F) immunoblot (n = 3/group), and (E) CM-H_2DCF-DA assay. To examine the effect of CO on the interaction between tubular cells and fibroblast cells under hypoxia condition, NRK-49F cells were treated with the supernatant from HK-2 cells, which was cultured with or without CORM-2 under hypoxia condition for 96 h, then analyzed by (G) immunoblot (n = 3/group). Results are expressed as the mean ± S.E.M.

schedule of CO-RBC administration to IR-AKI mice was set at 90 min before reperfusion (Fig. 4C). The amount of CO in the kidney 1 day after IR was significantly increased in the CO-RBC administration group (Fig. 4D). The IR-induced gene expression of the Kim-1 was reduced in the CO-RBC administration group (Fig. 4E). Consistent with this result, IR-induced levels of blood urea nitrogen (BUN) and serum creatinine (SCr) were significantly reduced in the CO-RBC administration group (Fig. 4F and G). We further conducted PAS and TUNEL staining to evaluate renal histology and apoptosis, respectively. The characteristic findings of renal injury such as the formation of columnar, tubular apoptosis were observed in the saline administration group, while CO-RBC administration improved such findings (Fig. 4H).

2.6. CO-RBC activates HIF-1α, AMPK and Nrf2 in IR-AKI

We assessed the protein levels of HIF-1α, VEGF and the phosphorylation of AMPK to confirm the renoprotective mechanism for how CO-RBC improved the pathological condition of IR-AKI. The administration of CO-RBC significantly upregulated the protein levels of these molecules as well as the levels of ATP compared with saline administration group (Fig. 5A and B). We next measured the antioxidant potential of CO-RBC. The administration of CO-RBC tended to increase

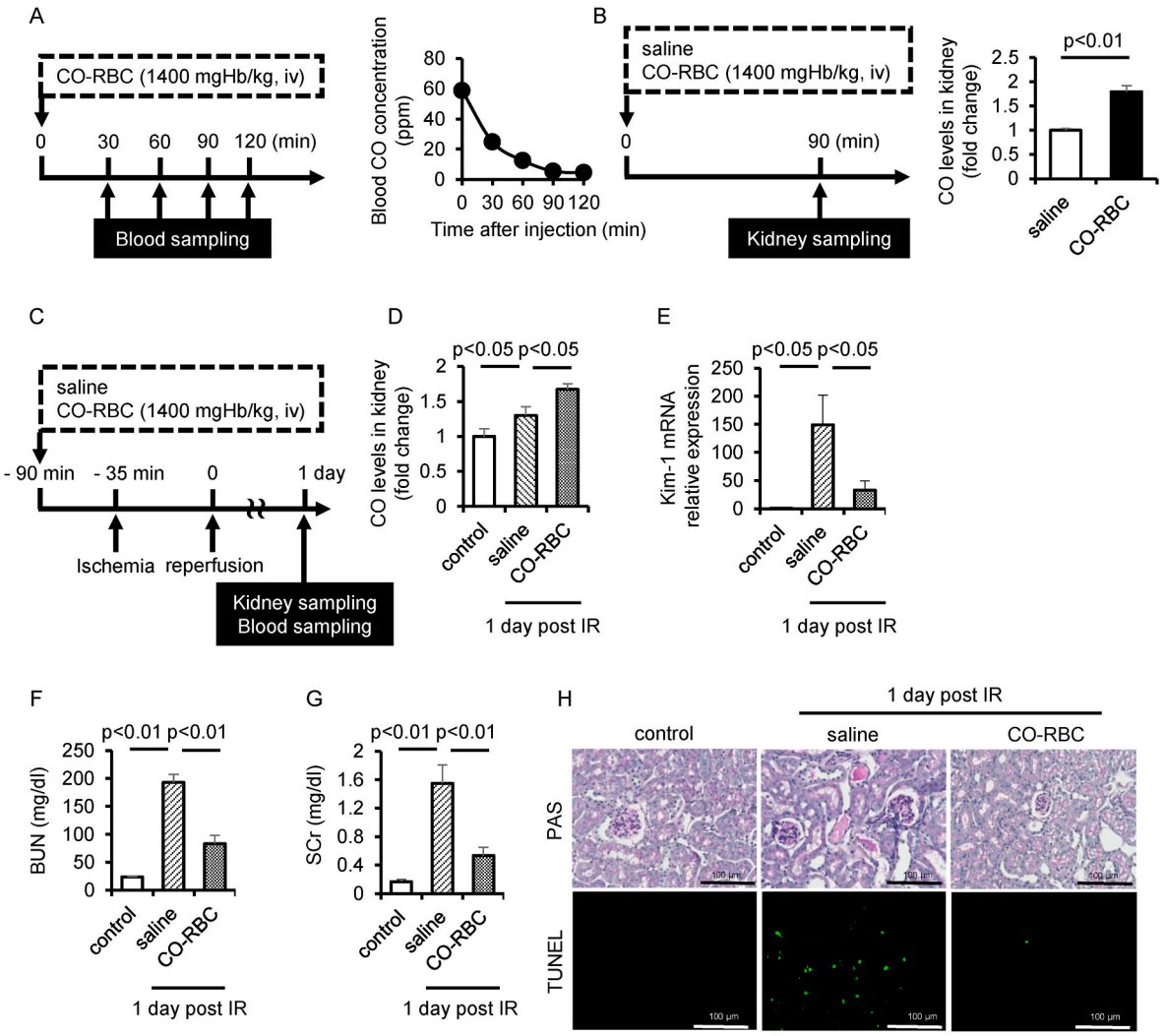

Fig. 4. CO-RBC exerts a renoprotective effect against IR-AKI. (A) A schematic summary of the schedule used for CO-RBC administration and blood sampling. CO concentrations in blood were measured by gas chromatography (n = 3/group). (B) A schematic summary of the schedule used for saline or CO-RBC administration and kidney sampling. CO concentrations in kidney were measured by gas chromatography (n = 4/group). (C) A schematic summary of the administration schedule used for saline of CO-RBC against IR-AKI. (D) CO concentrations in kidney were measured (n = 5/group). To evaluate the effect of CO on the tubular cell damage, the kidney was analyzed, (E) qRT-PCR (n = 5/group) combined with staining for (H) PAS and TUNEL. (F, G) To measure the kidney function, plasma levels of BUN and SCr were evaluated (n = 5/group). Results are expressed as the mean ± S.E.M.

protein levels of HO-1 and the nuclear translocation of Nrf2 (Fig. 5C and D). IR-induced renal NOX4 expression was significantly decreased in the CO-RBC administration group (Fig. 5C). We further performed immunostaining for 4-hydroxynonenal (4-HNE) and nitrotyrosine (NO-Tyr), markers for oxidative stress in renal tissue [54,55]. The positive areas in the vicinity of the tubules were elevated in the saline administration group, whereas CO-RBC administration resulted in a decrease in such areas (Fig. 5D). The plasma level of diacron-reactive oxygen metabolites (d-ROMs) is an oxidative stress biomarker for AKI [56]. Consistence with the results of immunostaining with 4-HNE, NO-Tyr in renal tissue, the IR-induced levels of d-ROMs in plasma were attenuated in the CO-RBC administration group (Fig. 5E).

2.7. CO-RBC suppresses inflammation in IR-AKI

We examined the anti-inflammatory effects of CO-RBC. IR-induced the gene expression of inflammatory cytokines, *i.e.*, TNF-α and IL-6, was decreased in the CO-RBC administration group (Fig. 5F and G). We further performed immunostaining for F4/80 (macrophages) and MPO (neutrophils) to assess the degree of infiltration of inflammatory cells. CO-RBC suppressed the IR-induced infiltration of these cells (Fig. 5I). The upregulation of the peroxisome growth factor-activating receptor γ (PPARγ) is partially attributed to the anti-inflammatory effects of CO [57]. The gene expression was significantly upregulated in the CO-RBC administration group (Fig. 5H).

2.8. CO-RBC improves renal fibrosis in IR-AKI to CKD

Three administrations of bardoxolone methyl, a Nrf2 activator, on every other day starting on 1 day after IR suppressed the pathological conditions of AKI to CKD [58]. Based on this administration schedule, we administered the CO-RBC (700 mgHb/kg, iv) to IR-AKI to CKD mice (Fig. 6A). Body weight loss is one of the physical findings that is typically observed during the acute exacerbation of CKD [59]. Although no variation in body weight was observed between the three groups 14 days after IR, the weight loss 7 days after IR was significantly suppressed in the CO-RBC administration group (Fig. 6B). Histopathological findings from PAS and TUNEL staining showed that the administration of CO-RBC improved the characteristic features of renal injury such as the development of columnar and tubular apoptosis (Fig. 6C). The staining of picrosirius red and masson's trichrome as well as the quantification of hydroxyproline showed that the AKI to CKD-induced accumulation of

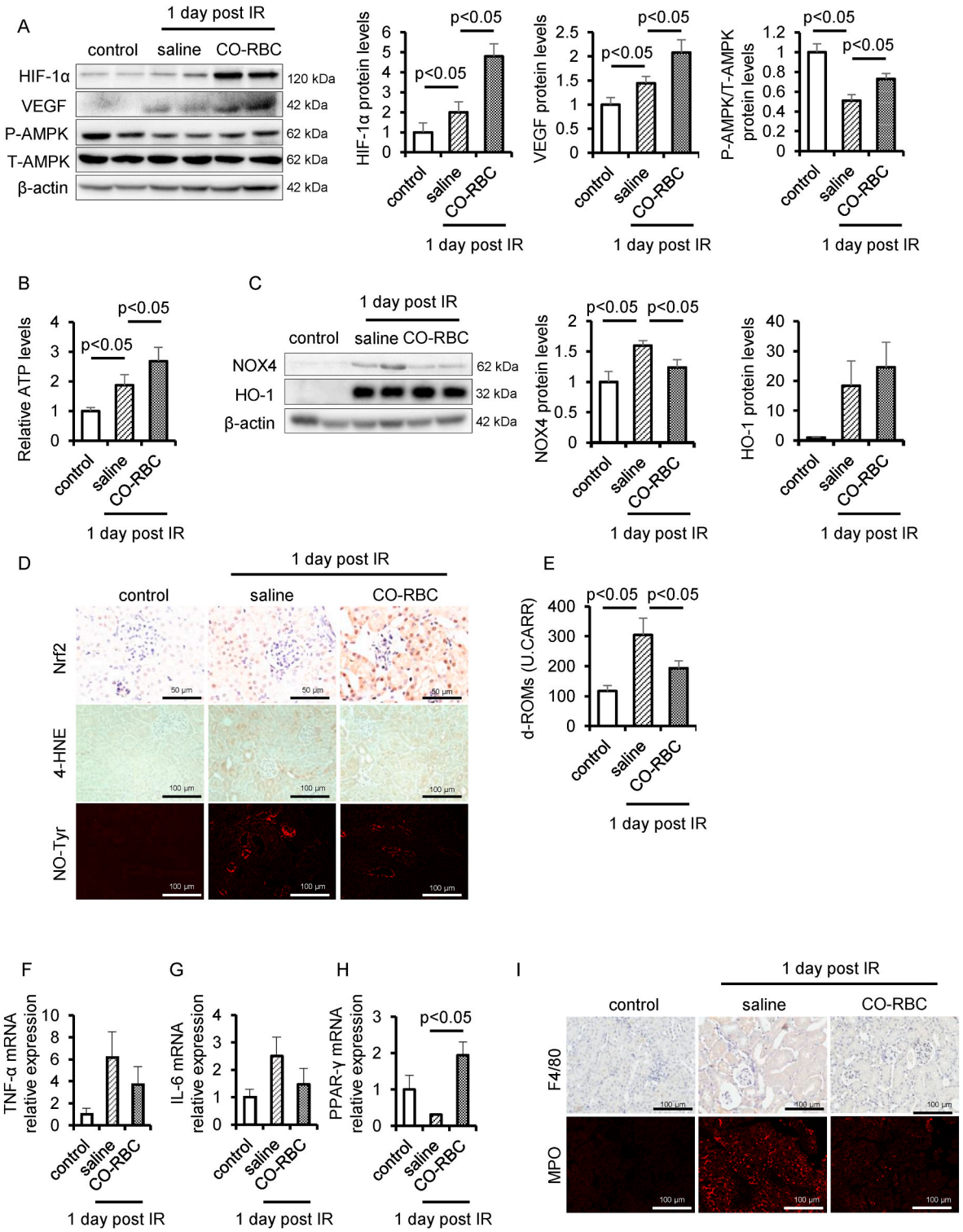

Fig. 5. CO-RBC activates HIF-1α, AMPK and Nrf2 against IR-AKI. To assess the hypoxia response, energy metabolism, redox balance and inflammation, kidney was collected 24 h after renal IR with or without CO-RBC treatment, then analyzed by (A, C) immunoblot (n = 5/group), (B) ATP assay (n = 5/group), (D, I) immunostaining, and (F–H) qRT-PCR. (n = 5/group). (E) The plasma level of d-ROMs was measured (n = 5/group). Results are expressed as the mean ± S.E.M.

collagen was reduced in the CO-RBC administration group (Fig. 6D and E). To examine the issue of whether CO-RBC exerted an antifibrotic effect via the suppression of EMT, we conducted immunostaining for E-Cadherin and α-SMA. A decreased E-Cadherin protein levels and elevated α-SMA protein levels was observed 14 days after IR, while these expression patterns were reversed in the CO-RBC administration group (Fig. 6F). Moreover, AKI to CKD-induced TGF-β1 was decreased in the CO-RBC administration group (Fig. 6F). Consistent with the immunostaining results, the analysis of western blot further confirmed that the expression pattern of α-SMA and TGF-β1 in the CO-RBC administration group (Fig. 6G).

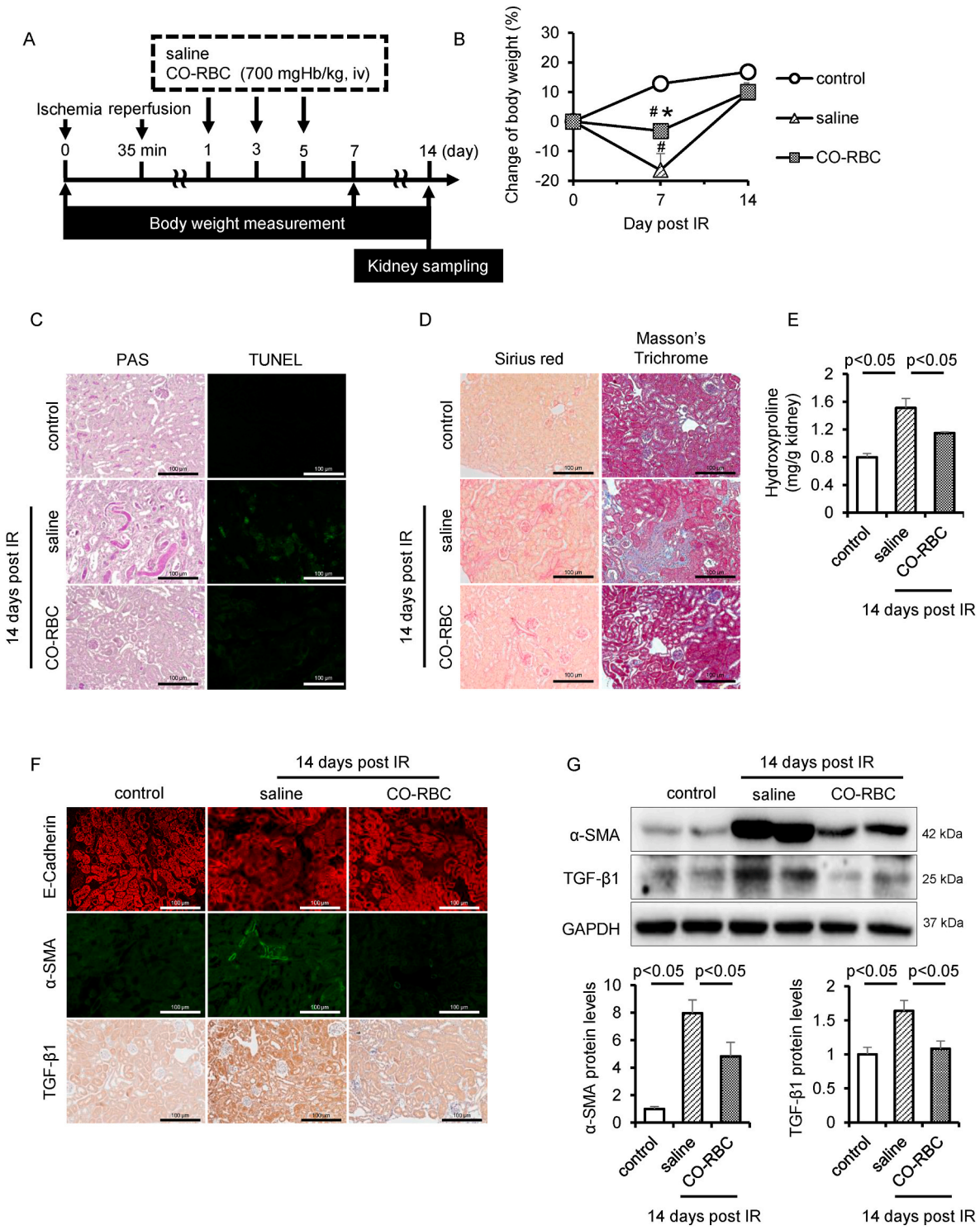

Fig. 6. CO-RBC exerts antifibrotic effect against IR-AKI to CKD. (A) A schematic summary of the administration schedule used for saline or CO-RBC against IR-AKI to CKD. (B) Weight fluctuations were monitored until 14 days after IR (n = 5/group). To assess the tubular cell damage, collagen accumulation and EMT pathway, kidney was collected 14 days after renal IR with or without CO-RBC treatment, then analyzed by (C) PAS and TUNEL staining, (D) picrosirius red and masson's trichrome staining, (E) quantification of hydroxyproline (n = 5/group), (F) immunostaining and (G) immunoblot (n = 5/group). Results are expressed as the mean ± S.E.M. $^{\#}p < 0.01$ compared with control group vs saline administration or CO-RBC administration group. $^{*}p < 0.05$ compared with saline administration group vs CO-RBC administration group. (For interpretation of the references to color in this figure legend, the reader is referred to the Web version of this article.)

2.9. CO-RBC regulates energy metabolism and oxidative stress in IR-AKI to CKD

HIF-1α is a renoprotective molecule that improves tissue hypoxia [13]. However, a constant expression of HIF-1α induces renal fibrosis via upregulating inflammatory gene expression [60]. Thus, we examined the issue of whether CO-RBC affects the HIF-1α protein levels in IR-AKI to CKD. The increased HIF-1α 14 days after IR was reduced in CO-RBC administration group (Fig. 7A). The protein levels of phosphorylation of AMPK and the levels of ATP were enhanced in the CO-RBC

administration group (Fig. 7A and B). Further, the elevated the number of Ki-67 positive cells, a marker of cell proliferation [61], 14 days after IR was reduced in the CO-RBC administration group (Fig. 7C). To examine the extent of oxidative stress in renal tissue, we conducted western blotting for NOX4 and HO-1, and immunostaining for Nrf2. The increased protein levels of these molecules 14 days after IR were reduced in the CO-RBC administration group (Fig. 7D). Consistent with these results, positive regions for 4-HNE and NO-Tyr were reduced in the

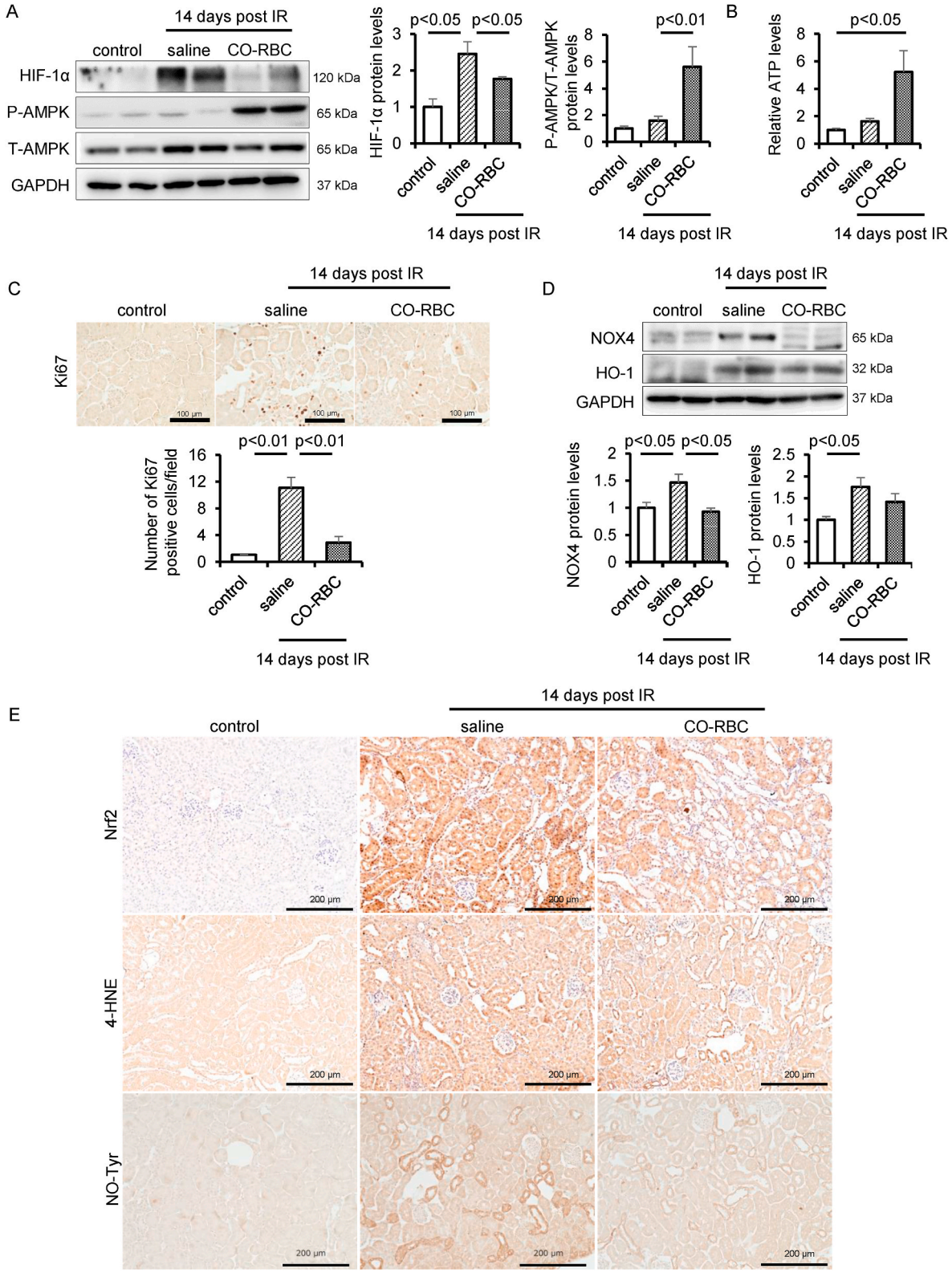

Fig. 7. CO-RBC maintains oxygen, redox and energy homeostasis in the kidney of IR-AKI to CKD. To investigate the effect of CO-RBC on the chronic hypoxia, disruption of energy metabolism, renal disorders, and renal redox balance, kidney was collected 14 days after renal IR with or without CO-RBC treatment, then analyzed by (A, D) immunoblot (n = 5/group), (B) ATP assay (n = 5/group), and (C, E) immunostaining. Results are expressed as the mean ± S.E.M.

CO-RBC administration group (Fig. 7E).

3. Discussion

We have previously demonstrated the therapeutic effect of CO-RBC on rhabdomyolysis- or crash syndrome-induced AKI model [38]. In this study, we report that CO-RBC prevents the progression to CKD from IR-induced AKI or AKI to CKD. Our data show the therapeutic mechanisms responsible for how the bioinspired CO delivery system supplies CO to tubular cells and subsequently suppresses hypoxia-induced cell damage via the activation of HIF-1α, AMPK and Nrf2 pathways.

The amount of CO was increased in the kidney from the IR-AKI mice with or without CO-RBC administration (Fig. 4D). Consistence with the report by Chen, H. et al. [62], we demonstrated that renal HO-1 was upregulated by IR (Fig. 5C). Since there is close correlation between the amount of CO and the protein levels of HO-1 [63], we speculated that the increased level of CO in the kidney is dependent on the IR-induced HO-1 protein levels. Although endogenous CO acts protectively against tubular cell damage, the saline administration group did not improve the pathological condition of IR-AKI under our experimental conditions (Fig. 4E–H). In contrast, the CO-RBC administration group showed a significant renoprotective effect on IR-AKI (Fig. 4E–H). These data indicate that the CO-RBC administration delivered a sufficient amount of CO into the kidney to allow for IR-induced tubular cell damage to be improved.

The findings reported herein demonstrate that CO-RBC is able to supply CO to the kidneys of mice at 1 day after reperfusion (Fig. 4D). Since IR damage occurs in the first few seconds or minutes after reperfusion, discussing the causal relationship between the presence of CO and the protection against IR-induced kidney damage based on our data which involves assessing the CO concentration in the kidney at 1 day after reperfusion would be insufficient. However, our current preliminary experiments clearly showed that the amount of CO in the kidney of healthy mice was increased at 90 min after CO-RBC administration (S. Fig. 3). In addition, the administration of only CO-RBC at 90 min before reperfusion had a renoprotective effect on IR-AKI (S. Fig. 4). These results suggest that CO-RBC has the potential to protect tubular cells from the damage that occurs immediately after reperfusion.

It is also necessary to consider the effects of carriers that deliver CO, such as iCORM-2 and RBC, on cells to demonstrate the authentic effects of CO. Wang, B. et al. reported that iCORM-2 exerts antioxidant activity by decomposing hydrogen peroxide as well as capturing free radicals in a cell free medium [64]. In contrast, we found that the renoprotective effect of CORM-2 against hypoxia-induced tubular cell damage, as evidenced by the gene expression of Kim-1, was completely abolished in the case of a combination with the CO scavenger, hemoCD (Fig. 3A). Considering that a pretreatment with the antioxidant, *N*-acetylcysteine, protects cells from the hypoxia-induced cell death [65], the major factor to evoke hypoxia-induced cell damage is assumed to be the generation of intracellular oxidative stress. These findings indicate that the antioxidant activity of iCORM-2 had a negligible effect on our *in vitro* experiment about the hypoxia-induced tubular cell damage.

We additionally conducted an experiment that was designed to confirm whether iCORM-2, which was prepared by the incubation of CORM-2 in DMSO for 18 h, was uncapable of releasing CO. Based on a report by Taguchi, K. et al. [66], a 1 ml portion of a 100 μM CORM-2 solution (DMSO) was sealed and incubated in a 10 ml vial under 5% CO_2 at 37 °C, and the concentration of CO in headspace of the vial was then measured by gas chromatography at each time point. The analysis showed that the concentration of CO in the headspace reached a plateau after a 4 h incubation, and that the value was constant for periods of up to 24 h (S. Fig. 5). Southam, M. et al. also showed that CO derived from the CORM-2 was nearly exhausted after a 4 h period of incubation in DMSO [67]. We further confirmed that the treatment of HK-2 cells with iCORM-2 did not activate HIF-1α, AMPK, and Nrf-2, all of which were activated by the CORM-2 treatment (S. Fig. 2A and B). We therefore concluded that the iCORM-2, which was used in our study, has no ability to release CO.

CO is produced in the process of heme metabolism by the action of HO-1 [21]. In addition, there is a close correlation between the amount of CO and the protein levels of HO-1 [63] since heme proteins, such as RBC, upregulate the protein levels of HO-1 [68], resulting in an enhancement in heme metabolism and the subsequent production of CO. To determine whether the CO liberated from CO-RBC is responsible for the increase in renal CO levels after the administration of CO-RBC, we first analyzed the kidneys of healthy mice at 90 min after the administration of saline or O_2-RBC or CO-RBC (S. Fig. 6A). In the case of the administration of O_2-RBC, the renal CO levels were significantly low compared with the data for the administration of CO-RBC (S. Fig. 6B). In addition, HIF-1α, AMPK and Nrf2 in the kidney were not activated at 6 h after the O_2-RBC administration (S. Fig. 6C–E). These results were confirmed by increased protein levels of VEGF and HO-1 in the kidney (S. Fig. 6D). We further confirmed that O_2-RBC had no therapeutic effect on impaired kidney function in IR-AKI mice (S. Fig. 7A–C). CO-RBC upregulated the renal protein levels of HIF-1α, VEGF, HO-1, and the phosphorylation of AMPK in IR-AKI mice, while O_2-RBC had no such ability (S. Fig. 7D). O_2-RBC also had no ability to downregulate IR-induced renal NOX4 expression (S. Fig. 7D). In addition, the nuclear translocation of Nrf2 was not increased by the administration of O_2-RBC (S. Fig. 7E). These findings suggest that the RBC (1400 mgHb/kg), which were used in our experimental conditions, is an insufficient amount to produce the CO in the kidney and to induce the downstream proteins of the CO signaling pathways. We therefore concluded that an increase in renal CO levels derived from CO-RBC exerted therapeutic effects on this type of kidney injury.

Regarding the IR-AKI to CKD mice, it is essential to clarify whether CO-RBC suppressed the progression to CKD independent of the onset of AKI. The pathological condition of AKI to CKD was suppressed by the administration of three doses of CO-RBC every other day starting 1 day after IR (Fig. 6). On the other hand, the pathological condition of AKI was not suppressed in the case of the administration of CO-RBC 60 min after IR (S. Fig. 4). This led us to conclude that the therapeutic intervention based on our administration schedule of CO-RBC clearly reflects the therapeutic effects on AKI to CKD without having any impact of the onset of AKI.

CO-RBC administration resulted in increased ATP production and caused a reduction in the number of Ki-67-positive cells in IR-AKI to CKD mice (Fig. 7A–C). The levels of ATP in damaged tubular cells determine the degree of renal pathology [12]. In fact, Suzuki, T. et al. reported that MA-5, a drug that causes an increase in ATP production, ameliorates IR-induced tubular cell damage [69]. Since there is a positive correlation between the number of Ki-67-positive cells and the degree of renal damage [70], we conclude that our data regarding the decrease in the number of Ki-67-positive cells confirms the renoprotective effect of CO-RBC.

Mitochondrial oxidative phosphorylation is known to be one of the representative ATP production pathways [71] and is positively regulated by AMPK [72]. Recent studies have revealed that CO can enhance oxidative phosphorylation in endothelial cells [73] and that it also has an effect on the activation of AMPK in embryonic fibroblasts [29]. However, no evidence has yet been made available concerning the mechanism by which CO promotes ATP production in tubular cells. The findings reported in this study show that a CO treatment activated AMPK and promoted the production of ATP, both in *in vitro* and *in vivo* (Figs. 2A, 3C, 5A and B, 7A and B). Therefore, our data points to the possibility that a part of the increase in ATP production is due to mitochondrial oxidative phosphorylation. On the other hand, it is also known that glycolysis is a mitochondria-independent pathway for ATP production [71] and is positively regulated by HIF-1α [74]. Consistent with previous report by Correa-Costa, M. et al. [75], CO upregulated the protein levels of renal HIF-1α (Fig. 5A). These findings indicate that CO also enhances ATP production via glycolysis. To clarify the effect of CO

on ATP production in more detail, additional experiments with the objective of evaluating the oxygen consumption rate [76], an indicator of mitochondrial oxidative phosphorylation, and the extracellular acidification rate [76], an indicator of glycolysis, will be needed in the future.

Sustained HIF-1α which is caused by chronic hypoxia in the kidney contributes to the development of CKD [77]. In fact, Li, L. et al. reported that the HIF-1α protein levels were enhanced at 1–2 weeks after IR in kidney [78]. The present study also provides data to show that IR-AKI to CKD mice showed a marked increase in renal HIF-1α (Fig. 7A). Meanwhile the protein levels were reduced in the CO-RBC administration group (Fig. 7A), but the mechanism responsible for this is unclear. Recent studies reported that CO has, not only vasodilatory effects via activation of soluble guanylate cyclase (sGC) [79], but also angiogenic effects via induction of HIF-1α/VEGF pathway [80]. Interestingly, an HIF-1α stabilizer improves renal hypoxia in the early-stage of CKD [81], and the sGC stimulator suppresses renal fibrosis [82]. Considering this body of evidence, coupled with our data showing that CO-RBC induced HIF-1α and VEGF protein levels in IR-AKI mice corresponding to the early-stage of CKD (Fig. 5A), it appears that CO-RBC improved the AKI-induced chronic hypoxia and decreased the protein levels of HIF-1α after ameliorating pathological conditions through vasodilatory and angiogenic effects of CO.

We demonstrate herein that Mito-TEMPO attenuated the protein levels of CO-induced HIF-1α in HK-2 cells, but not the CO-induced phosphorylation of AMPK or the nuclear translocation of Nrf2 (Fig. 1C and E). These results indicate that CO activates AMPK and Nrf2 and that this activation is independent of the mtROS pathway in HK-2 cells. Interestingly, we found that ATP production was slightly decreased in HK-2 cells 3 h after the CORM-2 treatment (S. Fig. 8). This characteristic result has also been reported for metformin [83]. Metformin can increase the AMP/ATP ratio through the transient suppression of the mitochondrial respiratory chain complex I, thereby inducing the AMPK phosphorylation and the nuclear translocation of Nrf2 [84]. Given that CO also can transiently inhibit the mitochondrial respiratory chain complex IV [85], CO may operate via a metformin-like mechanism in HK-2 cells.

The protein levels of NOX4 is increased under hypoxia condition via enhancing the secretion of TGF-β1[86] while NOX4-derived ROS induces the secretion of TGF-β1[87]. Therefore, hypoxia could be responsible for the positive feedback mechanism between TGF-β1 and NOX4. Hovater, M. et al. reported that CO attenuates the TGF-β1-induced activation of Smad by reducing the membrane expression of the TGF-β receptor in vascular smooth muscle cells [88]. Hemin, an HO-1 inducer, alleviates hypoxia-induced ROS [89]. In this study, we found that CORM-2 and CO-RBC induced Nrf2/HO-1 pathway, both *in vitro* and *in vivo*, respectively (Fig. 1A and B, 5C and D). We further found that treatment of HK-2 cells with CORM-2 under hypoxia condition reduced intracellular ROS levels and the protein levels of TGF-β1 and NOX4 (Fig. 3D–F). Accordingly, the suppressive effect of CO on the protein levels of NOX4 may be due not only to the reduction in membrane expression of the TGF-β1 receptor, but also to a decrease in TGF-β1 expression through the suppression of intracellular ROS via the CO-induced Nrf2/HO-1 pathway.

The increased TNF-α and IL-6 gene expression in IR-AKI mice was suppressed in the CO-RBC administration group (Fig. 5F and G). Of note, PPARγ gene expression significantly increased in this condition (Fig. 5H). Haschemi, A. et al. and Nizamutdinova, I. et al. reported that CO exerts an anti-inflammatory effect on macrophages [90] and endothelial cells [91] through the induction of PPARγ, respectively. On the other hand, Toll-like receptor (TLR) signaling is involved in the production of inflammatory cytokines such as TNF-α and IL-6. In a previous study, we reported that CO-RBC suppressed the extracellular leakage of HMGB-1, a TLR substrate, in a mouse model of acute liver injury [37]. Nakahira, K. et al. also reported that CO suppresses the translocation of TLR4 into lipid rafts in macrophages through the reduction of ROS production [92]. Thus, these collective findings show that CO exerts a direct or indirect anti-inflammatory effect via the induction of PPARγ or the attenuation of the TLR pathway, respectively.

Tissue hypoxia is also involved in fibroblast activation, which eventually leads to the development of renal fibrosis [93]. The HO-1 inducer improves myocardial fibrosis via the inhibition of fibroblast activation [94]. In the present study, a CORM-2 treatment under hypoxia condition not only elevated HO-1 protein levels but also suppressed the protein levels of α-SMA and COL1A1 (S. Fig. 9). Since CO has excellent cell membrane permeability, CO can easily gain access to cells regardless of the cell type. Based on this property, CO would be expected to exert a renoprotective effect via acting not only on tubular cells, which are the origin of renal pathology, but also on a variety of other cells such as fibroblasts and macrophages, both of which is attributed to the development of renal fibrosis.

Correa-Costa, M. et al. reported that the inhalation of 250 ppm CO for 1 h did not cause renal hypoxia in healthy mice [75]. In addition, Weideman, A. et al. applied a 1 h inhalation of 1000 ppm CO to create physiological hypoxia conditions [95]. Our present data show that the maximum blood concentration of CO after the administration of CO-RBC to healthy mice was 60 ppm, and this concentration decreased to the baseline value after 90 min of administration (Fig. 4A). Based on these data, CO-RBC administration would not be expected to cause renal hypoxia. However, an experiment showing whether CO-RBC cause renal hypoxia would be important in terms of understanding the mechanism responsible for how CO-RBC ameliorates the pathological conditions of AKI or AKI to CKD. In the future, experiments designed to evaluate whether or not CO-RBC has an effect on oxygen saturation and renal hypoxia in healthy mice will be needed using a pulse oximeter [96] and pimonidazole [97], respectively.

Since severe damage appears immediately after the onset of AKI, many cases in which the therapeutic agents were administrated after the onset resulted in an insufficient therapeutic effect on renal injury [58, 98–100]. In fact, in this study, we did not detect any renoprotective effects by the administration of CO-RBC, even at 60 min after reperfusion, corresponding to immediately after the onset of AKI (S. Fig. 4). On the other hand, we speculate that the pre-administration of CO-RBC could be used in AKI patients for which onset is predictable. For example, the incidence of ischemic AKI is 30% in cardiac surgery [101] and 20–80% for kidney transplantation [102]. These ischemic AKI induced by IR injuries occurs during some surgeries due to the temporary interruption of blood flow and reperfusion. Intriguingly, a phase III clinical trial is currently underway that is designed to prevent the onset of AKI by pre-administering QPI-1002, p53 siRNA, in cardiac surgery (https://clinicaltrials.gov/). In addition, Nakao, A. and co-workers et al. demonstrated that a CO treatment is effective in cases of kidney transplantation [103–106]. Based on these reports, we pre-administered CO-RBC to IR-AKI mice in our study (Fig. 4C). These findings serve to confirm that our study more closely mimics a clinical situation.

Vera, T. et al., in an *in vivo* study, showed that a CO donor ameliorated the kidney injury induced by ischemic AKI [99]. They only discussed the potential effect of HO-1 induced by a CO donor as the therapeutic mechanism. In the present study, we demonstrated that CO-RBC activated, not only HO-1, but also HIF-1α, AMPK and Nrf2 in kidney or tubular cells (Fig. 5A and D, S. Fig. 1E and F). Moreover, the data reported in this study points to the possibility that these proteins improved the pathological condition of not only IR-AKI, but also IR-AKI to CKD. Thus, our study provides a better understanding of the therapeutic mechanism for how CO ameliorates kidney injury.

Nakao, A. and colleagues et al. reported on the protective effect of CO on a model of kidney transplantation-induced IR injury [103–106]. Consistent with their reports, CO-RBC improved the conditions associated with IR-AKI (Fig. 4C–H). It should, however, be noted that there are differences in the animal species and pathological models between our experiments and theirs, these findings indicate that CO-RBC has a pharmacological effect that is comparable to those of other CO

applications. Nakao, A. and colleagues et al. utilized CO inhalation and *ex vivo* CO exposure as a method for administering CO [103–106]. Based on these reports, clinical trials of CO inhalation for kidney transplantation have been conducted (https://clinicaltrials.gov/). However, CO has not yet been used in clinical practice. One possible reason for this is that these methods that are used to deliver CO have limitations in that hospitals would need specific equipment and specialists to avoid respiratory depression. To overcome this limitation, we used CO-RBC for this delivery, because CO-RBC can be easily prepared by exposing purified RBC to CO gas for a period of 10 min, and the dosage of CO can be easily adjusted based on the amount of hemoglobin in the sample. In addition, CO-RBC would be expected to function as an O_2 carrier after the dissociation of CO from the hemoglobin of RBC. In fact, CO-RBC reduced the extent of lethality in rats with massive hemorrhagic shock and this reduction was equivalent to that for O_2-RBC [39]. We also confirmed that no respiratory depression due to CO-RBC administration was detected in the present study. Therefore, we believe that CO-RBC has the potential for being used to deliver CO in a clinical setting and that no specialized equipment would be needed to achieve this.

Experiments using CO gas is the best way to demonstrate the actual effects of CO. However, the current study was aimed at establishing another clinically applicable CO preparation method due to several limitations with the clinical use of CO gas. Therefore, we established CO-RBC and designed *in vitro* or *in vivo* experiments using iCORM-2 or O_2-RBC as a negative control, respectively, to investigate the rigorous effects of CO (S. Figs. 2, 6 and 7). Our findings clearly showed that CO contributed to the activation of HIF-1α, AMPK, and Nrf-2, and the subsequent pharmacological effect on IR-induced AKI. Given that levels of oxygen saturation which is defined as the ratio of oxy-hemoglobin to the total concentration of hemoglobin are about 95% or more in normal mice [107], the difference in pharmacological effects between RBC and O_2-RBC would be predicted to be negligible.

4. Conclusion

In this study, we demonstrate that CO-RBC improves the pathological conditions associated with AKI and AKI to CKD. Our bioinspired CO delivery system has the potential for serving as an effective cell therapy for the progression to CKD regardless of the primary disease.

5. Materials and methods

5.1. Cell and treatment

HK-2 and NRK-49F cells were bought from American Tissue Type Culture Collection (Manassas, VA, USA). The cells were grown in DMEM/F12 (Wako Pure Chemical, Ltd., Wako, Osaka, Japan) supplemented with 10% fetal bovine serum (FBS, Invitrogen, Carlsbad, CA, USA), penicillin (100 U/ml, Invitrogen), and streptomycin (100 μg/ml, Invitrogen). Culture conditions were maintained at 37 °C in a humidified atmosphere at 5% CO_2. HK-2 cells were treated with CORM-2 (Sigma-Aldrich, Sigma, St. Louis, MO, USA) and Mito-TEMPO (Sigma) to examine the effect of CO-driven mtROS on the activation of HIF-1α, AMPK and Nrf2. For exposing HK-2 or NRK-49 cells to hypoxia, the cells were incubated in a hypoxia chamber (0.1% O_2, 5% CO_2 and 94% N_2) (Mitsubishi Gas Chemical Co. Inc., Tokyo, Japan), and treated with O_2-RBC, CO-RBC, CORM-2 and hemoCD (Doshisha University, Kyoto, Japan). Inactive CORM-2 (iCORM-2) was prepared as described by Sawle, P. et al. [108]. Briefly, CORM-2 was dissolved in DMSO for 18 h at 37 °C in a 5% CO_2 humidified atmosphere to liberate CO.

5.2. Western blotting

The lysate of cells and kidney tissues were prepared in a Mammalian Protein Extraction Reagent (M-PER, Thermo Fisher Scientific, Thermo, Waltham, MA, USA) in the presence of a protease inhibitor (1:100, Nacalai Tesque, Kyoto, Japan) and a phosphatase inhibitor (1:100, Nacalai Tesque). The samples were centrifuged at 12,000 rpm for 10 min at 4 °C, then the quantification of protein was implemented by a BCA protein assay (Wako). Protein (30 μg) were applied to SDS-PAGE 10%, followed by transfer to Immobilon-P (0.45 μm, Millipore, Temecula, CA, USA). Primary antibodies were added followed by secondary antibodies. After reaction with SuperSignal West Pico substrate (Thermo) or ImmunoStar LD (Wako), the images of visualized protein were acquired using a FUSION (Vilber Lourmat, Marne-laf-Vallée, France). The data were quantified using ImageJ Fiji software. β-actin or GAPDH was used for loading controls. The primary and secondary antibodies are provided in Supplemental Table 1.

5.3. Immunostaining analysis

HK-2 cells were fixed using 4% paraformaldehyde, followed by permeabilization using 0.3% TritonX-100 in PBS at room temperature (RT) for 30 min. Next, the cells were blocked with PBS containing 1% BSA at RT for 30 min, then reacted with an anti-Nrf2 (1:50, Abcam, ab31163) antibody overnight at 4 °C. The cells were incubated at 37 °C for 1 h with Alexa Fluor 647 anti-rabbit IgG antibody (H + L) (1:200, Invitrogen, A-21443) and DAPI (1:100, Dojindo Lab, Kumamoto, Japan). Immunofluorescent or immunohistochemical staining was performed to paraffin embedded-kidney sections. To immunofluorescently stain with anti-Nitrotyrosine (NO-Tyr, 1:50, Merck Millipore, AB5411, Burlington, MA, USA), MPO heavy chain (1:50, Santa Cruz, sc-16128-R), E-Cadherin (1:50, R&D Systems, ab5694, Minneapolis, MN, USA), and α-SMA antibodies, antigen retrieval was conducted by HistoVT One (Nacalai Tesque) at 95 °C for 30 min. To permeabilize the antibodies, the sections were reacted with 50 mM Tris/HCl plus 0.1% Tween-20 (T-TB), then conducted blocking using 4% Block Ace (KAC, Kyoto, Japan) at 37 °C for 30 min. The kidney sections were reacted with the primary antibody overnight at 4 °C, then washed with T-TB, followed by reaction with Alexa Fluor 647 anti-rabbit IgG antibody (H + L) or Alexa Fluor 647 anti-goat IgG antibody (H + L) (1:200, Invitrogen, A-21447) at RT for 1.5 h. To perform the immunohistochemical staining with anti-Ki-67 (1:50, CST, 12202), 4-hydroxynonenal (4-HNE, 1:50, Bioss Antibodies, bs-6313R, Woburn, MA, UA), F4/80 (1:50, Thermo, 14-4801-82), NO-Tyr, Nrf2 and TGF-β1 antibodies, antigen was retrieved. The kidney sections were reacted with 3% H_2O_2/methanol solution at RT for 30 min to inhibit endogenous peroxidase and were reacted with the primary antibody overnight at 4 °C. The kidney sections were then reacted with peroxidase-conjugated anti-rabbit IgG or anti-rat IgG antibody (Histofine Simple Stain MAX-PO, Nichirei Biosciences, Tokyo, Japan) at RT for 30 min, followed by reaction with DAB solution at RT for 3 min. All images of slides were acquired with a BZ-X710 (Keyence, Osaka, Japan). The positive cells number of Ki-67 were qualified in an area of 270 × 360 μm (original magnification, x400). At minimum ten areas of kidney specimens from each mouse were used in the analysis.

5.4. Quantitative real-time polymerase chain reaction (qRT-PCR) analysis

The gene expression of Kim-1, TNF-α, and IL-6 were measured by qRT-PCR. All primers were purchased from Takara Bio (Tokyo, Japan). The RNA extracted from HK-2 cells and kidney was prepared using RNAiso plus (Takara Bio), then reverse transcribed by means of PrimeScript RT Master Mix (Takara Bio). After reaction with SYBR Premix Ex Taq II (Takara Bio), qRT-PCR was conducted with an iCycler thermal cycler (Bio-Rad, Hercules, CA, USA). The qRT-PCR method has been previously described [109]. GAPDH was used as an internal control. The sequences of the oligonucleotide primers are provided in Supplemental Table 2.

5.5. Cell viability assay

The rate of living cells was qualified by means of a Cell Counting Kit-8 (CCK-8) assay (Dojindo Lab). HK-2 cells were incubated in 96-well with or without CORM-2 (100 μM) under hypoxia condition for 96 h. After adding CCK-8 reagent, the 96-well was maintained at 37 °C for 2 h. To acquire the absorbance at 450 nm, a Microplate reader (Bio Rad) was used.

5.6. ATP assay

Intracellular ATP levels in HK-2 cells and kidney were determined by means of an ATP assay kit (Cosmo Bio). Cell or tissue was treated with ATP extraction reagents. After the extracted solution was reacted with the luminescent reagent, the luminescence intensity was measured with a luminometer (Promega, Madison, WI, USA). Each ATP levels per protein was standardized by the value of control group.

5.7. Measurement of ROS

Intracellular ROS levels in the HK-2 cells were measured by a CM-H_2DCF-DA probe (Thermo). HK-2 cells were grown on a glass-base dish (IWAKI, Shizuoka, Japan) with or without CORM-2 under hypoxia condition for 48 h. The culture media was replaced with D-PBS containing 2 μM CM-H_2DCF-DA and incubated at 37 °C for 30 min. After incubation, stained cells were observed by BZ-X710.

5.8. Animals

ICR mice (male, 6 weeks, 20–24 g, SLC Japan, Inc., Shizuoka, Japan) were used for all experiments, and the animals were housed in a room with food and drinking water on a 12-h light/dark cycle while maintaining a temperature (18–24 °C) and a relative humidity (40–70%). All animal experiments were approved by the Animal Experiments Committee of Kumamoto University and were conducted in accordance with the National Institutes of Health (NIH).

5.9. Preparation of O_2-RBC and CO-RBC

The solution of O_2-RBC and CO-RBC were purified as described in a previous report [39].

5.10. Quantification of CO amount in blood and kidney

To perfectly dissociate CO from Hb or hemoprotein, blood (0.02 ml) and kidney (whole kidney) samples were mixed with PBS (0.48 ml) containing saponin (0.01 ml, 16.7 mg/ml, Nacalai Tesque) or saponin (5 ml) in a vial (10 ml), respectively. Blood and kidney samples were incubated for 2 or 4 h respectively. The concentration of CO in headspace of vial was qualified by gas chromatography with a TRIlyzer mBA-3000 (Taiyo Instruments, Inc., Osaka, Japan).

5.11. Experimental procedure for IR-AKI or IR-AKI to CKD mice

IR model mice were prepared in a procedure based on the previous reports [110]. Body temperature was maintained at 37 °C during the procedure. To clamp both renal pedicles for 35 min, midline abdominal incision was conducted. After the clamping, occlusion of blood flow was confirmed by monitoring renal color change.

To examine the validity of the AKI model, the ischemic duration was set at 35 min and BUN as an index of renal function was measured at each time point (0, 1, 3, 12, and 24 h) after IR (S. Fig. 10). BUN levels showed a significant increase 24 h after IR, so the reperfusion duration was set at 24 h. CO-RBC was administrated (1400 mgHb/kg, iv) to IR-AKI mice 90 mine before reperfusion (Fig. 4C).

To investigate the renoprotective effects of CO-RBC on AKI to CKD, we first determined when renal fibrosis is detected after IR-induced AKI. When the levels of BUN decreased near the base line 14 days after IR (S. Fig. 11A), picrosirius red and masson's trichrome staining, both of which are used to detect collagen, showed evidence for interstitial fibrosis in renal tissue (S. Fig. 11B). These data were corroborated by the contents of renal hydroxyproline which is a main component of collagen (S. Fig. 11C). Thus, evaluation points for renal fibrosis were set at 14 days after IR. CO-RBC was administrated (700 mgHb/kg, iv) three times to IR-AKI to CKD mice on every other day starting on the first day after IR (Fig. 6A).

5.12. Analysis of renal function

To obtain plasma samples, blood samples from mice were centrifuged at 6000 rpm for 10 min at RT and the supernatant was then collected. Plasma levels of BUN and SCr were examined with FUJI DRI-CHEM 7000 (FUJIFILM, Tokyo, Japan).

5.13. Histological assessment of renal tissue

To dehydrate, 10% phosphate buffered formalin-fixed kidney tissues were processed with various concentration of ethyl alcohol. Kidney sections embedded in paraffin were prepared at 2 μm. Morphologic assessment was performed by staining of periodic acid-Schiff (PAS), picrosirius red, and masson's trichrome. Stained sections were observed with a BZ-X710.

5.14. d-ROMs test

The d-ROMs level in plasma was measured using an analyzer of free radical (FREE carpe diem, Wismerll, Tokyo, Japan).

5.15. TUNEL staining

Kidney sections were stained with TUNEL reagent (Roche, Basel, Switzerland) for the *in situ* detection of apoptosis. The sections were also stained with DAPI. The image of slides was obtained using BZ-X710.

5.16. Quantification of hydroxyproline levels in the kidney

Kidney was removed from mice 14 days after IR, and 5% trichloroacetic acid in milli-Q water was added for homogenization. After placing the samples on ice for 20 min, the supernatant was removed by centrifugation at 10,000 rpm for 4 °C at 10 min. The pellet was incubated with 10 N HCl at 110 °C for 12 h. The dried pellets were resuspended in milli-Q. The resulting suspension was incubated with a solution of chloramine-T (1.4% chloramine T, 4.1% sodium acetate, 10% Isopropanol) for 20 min at RT and Ehrlich's reagent for 15 min at 65 °C. The absorbance at 540 nm as a content of hydroxyproline was acquired with a Microplate reader (Bio Rad).

5.17. Statistics

The data are expressed as the mean ± SE. Two group data were compared using the Student's t-test. More than two groups were compared using analysis one-way ANOVA followed by Tukey's multiple comparison.

Author contributions

H.W. and T.M. conceived the research studies. T.N., H.M., H.Y., K.N., K.K., N.W., I.N., and R.M. conducted experiments and acquired data. H. S. and H.K. contributed to new reagents and analysis. T.N., H.M and T. M. wrote the paper. K.T., J.S., and M.O. critically reviewed the data and manuscript. H.M., H.W., and T.M. supervised the project.

Declaration of competing interest

The authors declare no competing interests.

Acknowledgements

This work was partially supported by a Grant-in-Aid for Young Scientists (B) (JP17K15511); and a Grant-in-Aid for Scientific Research (B) (JP18H02604) from Japan Society for the Promotion of Science , Japan.

Appendix A. Supplementary data

Supplementary data to this article can be found online at https://doi.org/10.1016/j.redox.2022.102371.

References

[1] O. Devuyst, et al., Autosomal dominant tubulointerstitial kidney disease, Nat. Rev. Dis. Prim. 5 (2019) 60, https://doi.org/10.1038/s41572-019-0109-9.
[2] R. Kazancioğlu, Risk factors for chronic kidney disease: an update, Kidney Int. Suppl. (2011) (3) (2013) 368–371, https://doi.org/10.1038/kisup.2013.79.
[3] G.C.K.D. Collaboration, Global, regional, and national burden of chronic kidney disease, 1990-2017: a systematic analysis for the Global Burden of Disease Study 2017, Lancet 395 (2020) 709–733, https://doi.org/10.1016/S0140-6736(20)30045-3.
[4] K. Makris, L. Spanou, Acute kidney injury: definition, pathophysiology and clinical phenotypes, Clin. Biochem. Rev. 37 (2016) 85–98.
[5] K. Takaori, et al., Severity and frequency of proximal tubule injury determines renal prognosis, J. Am. Soc. Nephrol. 27 (2016) 2393–2406, https://doi.org/10.1681/ASN.2015060647.
[6] C.V. Thakar, A. Christianson, J. Himmelfarb, A.C. Leonard, Acute kidney injury episodes and chronic kidney disease risk in diabetes mellitus, Clin. J. Am. Soc. Nephrol. 6 (2011) 2567–2572, https://doi.org/10.2215/CJN.01120211.
[7] J. Cerdá, et al., Epidemiology of acute kidney injury, Clin. J. Am. Soc. Nephrol. 3 (2008) 881–886, https://doi.org/10.2215/CJN.04961107.
[8] S.G. Coca, S. Singanamala, C.R. Parikh, Chronic kidney disease after acute kidney injury: a systematic review and meta-analysis, Kidney Int. 81 (2012) 442–448, https://doi.org/10.1038/ki.2011.379.
[9] D.A. Ferenbach, J.V. Bonventre, Mechanisms of maladaptive repair after AKI leading to accelerated kidney ageing and CKD, Nat. Rev. Nephrol. 11 (2015) 264–276, https://doi.org/10.1038/nrneph.2015.3.
[10] A. Ishani, et al., The magnitude of acute serum creatinine increase after cardiac surgery and the risk of chronic kidney disease, progression of kidney disease, and death, Arch. Intern. Med. 171 (2011) 226–233, https://doi.org/10.1001/archinternmed.2010.514.
[11] S. Shu, et al., Hypoxia and hypoxia-inducible factors in kidney injury and repair, Cells 8 (2019), https://doi.org/10.3390/cells8030207.
[12] S. Yamamoto, et al., Spatiotemporal ATP dynamics during AKI predict renal prognosis, J. Am. Soc. Nephrol. 31 (2020) 2855–2869, https://doi.org/10.1681/asn.2020050580.
[13] H. Li, Z. Xia, Y. Chen, D. Qi, H. Zheng, Mechanism and therapies of oxidative stress-mediated cell death in ischemia reperfusion injury, Oxid. Med. Cell. Longev. 2018 (2018), 2910643, https://doi.org/10.1155/2018/2910643.
[14] M. Jiang, et al., Mitochondrial dysfunction and the AKI-to-CKD transition, Am. J. Physiol. Ren. Physiol. 319 (2020) F1105–f1116, https://doi.org/10.1152/ajprenal.00285.2020.
[15] Y. Fang, H. Zhang, Y. Zhong, X. Ding, Prolyl hydroxylase 2 (PHD2) inhibition protects human renal epithelial cells and mice kidney from hypoxia injury, Oncotarget 7 (2016) 54317–54328, https://doi.org/10.18632/oncotarget.11104.
[16] P.W. Seo-Mayer, et al., Preactivation of AMPK by metformin may ameliorate the epithelial cell damage caused by renal ischemia, Am. J. Physiol. Ren. Physiol. 301 (2011) F1346–F1357, https://doi.org/10.1152/ajprenal.00420.2010.
[17] C. Diao, et al., Inhibition of PRMT5 attenuates oxidative stress-induced pyroptosis via activation of the Nrf2/HO-1 signal pathway in a mouse model of renal ischemia-reperfusion injury, Oxid. Med. Cell. Longev. 2019 (2019), 2345658, https://doi.org/10.1155/2019/2345658.
[18] Y. Wang, et al., A dual AMPK/Nrf2 activator reduces brain inflammation after stroke by enhancing microglia M2 polarization, Antioxidants Redox Signal. 28 (2018) 141–163, https://doi.org/10.1089/ars.2017.7003.
[19] I.J. Davies, Two cases of erythema due to carbon monoxide poisoning, Proc. Roy. Soc. Med. 7 (1914) 237–238.
[20] J.B. Haldane, Carbon monoxide as a tissue poison, Biochem. J. 21 (1927) 1068–1075, https://doi.org/10.1042/bj0211068.
[21] D. Boehning, S.H. Snyder, Circadian rhythms. Carbon monoxide and clocks, Science 298 (2002) 2339–2340, https://doi.org/10.1126/science.1080339.
[22] M. Zhuo, S.A. Small, E.R. Kandel, R.D. Hawkins, Nitric oxide and carbon monoxide produce activity-dependent long-term synaptic enhancement in hippocampus, Science 260 (1993) 1946–1950, https://doi.org/10.1126/science.8100368.
[23] A. Kobayashi, et al., Synergetic antioxidant and vasodilatory action of carbon monoxide in angiotensin II - induced cardiac hypertrophy, Hypertension 50 (2007) 1040–1048, https://doi.org/10.1161/HYPERTENSIONAHA.107.097006.
[24] R. Tenhunen, H.S. Marver, R. Schmid, The enzymatic conversion of heme to bilirubin by microsomal heme oxygenase, Proc. Natl. Acad. Sci. U. S. A. 61 (1968) 748–755, https://doi.org/10.1073/pnas.61.2.748.
[25] B.Y. Chin, et al., Hypoxia-inducible factor 1alpha stabilization by carbon monoxide results in cytoprotective preconditioning, Proc. Natl. Acad. Sci. U. S. A. 104 (2007) 5109–5114, https://doi.org/10.1073/pnas.0609611104.
[26] Y.K. Choi, et al., Carbon monoxide potentiation of L-type Ca(2+) channel activity increases HIF-1α-Independent VEGF expression via an AMPKα/SIRT1-mediated PGC-1α/ERRα Axis, Antioxidants Redox Signal. 27 (2017) 21–36, https://doi.org/10.1089/ars.2016.6684.
[27] Y.K. Choi, et al., Carbon monoxide promotes VEGF expression by increasing HIF-1alpha protein level via two distinct mechanisms, translational activation and stabilization of HIF-1alpha protein, J. Biol. Chem. 285 (2010) 32116–32125, https://doi.org/10.1074/jbc.M110.131284.
[28] H.J. Kim, et al., Carbon monoxide protects against hepatic steatosis in mice by inducing sestrin-2 via the PERK-eIF2α-ATF4 pathway, Free Radic. Biol. Med. 110 (2017) 81–91, https://doi.org/10.1016/j.freeradbiomed.2017.05.026.
[29] D. Stucki, et al., Carbon monoxide exposure activates ULK1 via AMPK phosphorylation in murine embryonic fibroblasts, Int. J. Vitam. Nutr. Res. 1–10 (2021), https://doi.org/10.1024/0300-9831/a000714.
[30] S. Kaiser, L. Selzner, J. Weber, N. Schallner, Carbon monoxide controls microglial erythrophagocytosis by regulating CD36 surface expression to reduce the severity of hemorrhagic injury, Glia 68 (2020) 2427–2445, https://doi.org/10.1002/glia.23864.
[31] P.L. Chi, C.C. Lin, Y.W. Chen, L.D. Hsiao, C.M. Yang, CO induces Nrf2-dependent heme oxygenase-1 transcription by cooperating with Sp1 and c-Jun in rat brain astrocytes, Mol. Neurobiol. 52 (2015) 277–292, https://doi.org/10.1007/s12035-014-8869-4.
[32] S. Qin, et al., Nrf2 is essential for the anti-inflammatory effect of carbon monoxide in LPS-induced inflammation, Inflamm. Res. 64 (2015) 537–548, https://doi.org/10.1007/s00011-015-0834-9.
[33] R.F. Coburn, A possible carbon monoxide shuttle in the lung, J. Appl. Physiol. (1985) 121 (2016) 558–567, https://doi.org/10.1152/japplphysiol.00184.2016.
[34] T. Sjostrand, Endogenous formation of carbon monoxide; the CO concentration in the inspired and expired air of hospital patients, Acta Physiol. Scand. 22 (1951) 137–141, https://doi.org/10.1111/j.1748-1716.1951.tb00762.x.
[35] Q. Mao, et al., Sensitive quantification of carbon monoxide in vivo reveals a protective role of circulating hemoglobin in CO intoxication, Commun. Biol. 4 (2021) 425, https://doi.org/10.1038/s42003-021-01880-1.
[36] S. Ogaki, K. Taguchi, H. Watanabe, M. Otagiri, T. Maruyama, Carbon monoxide-bound red blood cells protect red blood cell transfusion-induced hepatic cytochrome P450 impairment in hemorrhagic-shock rats, Drug Metab. Dispos. 41 (2013) 141–148, https://doi.org/10.1124/dmd.112.048744.
[37] S. Ogaki, et al., Kupffer cell inactivation by carbon monoxide bound to red blood cells preserves hepatic cytochrome P450 via anti-oxidant and anti-inflammatory effects exerted through the HMGB1/TLR-4 pathway during resuscitation from hemorrhagic shock, Biochem. Pharmacol. 97 (2015) 310–319, https://doi.org/10.1016/j.bcp.2015.07.035.
[38] K. Taguchi, et al., Carbon monoxide rescues the developmental lethality of experimental rat models of rhabdomyolysis-induced acute kidney injury, J. Pharmacol. Exp. Therapeut. 372 (2020) 355–365, https://doi.org/10.1124/jpet.119.262485.
[39] S. Ogaki, et al., Carbon monoxide-bound red blood cell resuscitation ameliorates hepatic injury induced by massive hemorrhage and red blood cell resuscitation via hepatic cytochrome P450 protection in hemorrhagic shock rats, J. Pharm. Sci. 103 (2014) 2199–2206, https://doi.org/10.1002/jps.24029.
[40] S.L. Saraf, et al., Genetic variants and cell-free hemoglobin processing in sickle cell nephropathy, Haematologica 100 (2015) 1275–1284, https://doi.org/10.3324/haematol.2015.124875.
[41] R. Motterlini, et al., Carbon monoxide-releasing molecules: characterization of biochemical and vascular activities, Circ. Res. 90 (2002) E17–E24, https://doi.org/10.1161/hh0202.104530.
[42] X. Song, Z. Gong, K. Liu, J. Kou, B. Liu, Baicalin combats glutamate excitotoxicity via protecting glutamine synthetase from ROS-induced 20S proteasomal degradation, Redox Biol. 34 (2020), 101559, https://doi.org/10.1016/j.redox.2020.101559.
[43] W.K. Han, V. Bailly, R. Abichandani, R. Thadhani, J.V. Bonventre, Kidney Injury Molecule-1 (KIM-1): a novel biomarker for human renal proximal tubule injury, Kidney Int. 62 (2002) 237–244, https://doi.org/10.1046/j.1523-1755.2002.00433.x.
[44] H. Kitagishi, et al., Feedback response to selective depletion of endogenous carbon monoxide in the blood, J. Am. Chem. Soc. 138 (2016) 5417–5425, https://doi.org/10.1021/jacs.6b02211.
[45] K. Fujii, et al., Xanthine oxidase inhibitor ameliorates postischemic renal injury in mice by promoting resynthesis of adenine nucleotides, JCI Insight 4 (2019), https://doi.org/10.1172/jci.insight.124816.
[46] D.G. Hardie, F.A. Ross, S.A. Hawley, AMPK: a nutrient and energy sensor that maintains energy homeostasis, Nat. Rev. Mol. Cell Biol. 13 (2012) 251–262, https://doi.org/10.1038/nrm3311.
[47] D.D. Zhang, et al., Carbon monoxide attenuates high salt-induced hypertension while reducing pro-inflammatory cytokines and oxidative stress in the paraventricular nucleus, Cardiovasc. Toxicol. 19 (2019) 451–464, https://doi.org/10.1007/s12012-019-09517-w.

[48] M. Sedeek, R. Nasrallah, R.M. Touyz, R.L. Hébert, NADPH oxidases, reactive oxygen species, and the kidney: friend and foe, J. Am. Soc. Nephrol. 24 (2013) 1512–1518, https://doi.org/10.1681/asn.2012111112.

[49] K.H. Sun, Y. Chang, N.I. Reed, D. Sheppard, α-Smooth muscle actin is an inconsistent marker of fibroblasts responsible for force-dependent TGFβ activation or collagen production across multiple models of organ fibrosis, Am. J. Physiol. Lung Cell Mol. Physiol. 310 (2016) L824–L836, https://doi.org/10.1152/ajplung.00350.2015.

[50] S.H. Han, et al., Deletion of Lkb1 in renal tubular epithelial cells leads to CKD by altering metabolism, J. Am. Soc. Nephrol. 27 (2016) 439–453, https://doi.org/10.1681/asn.2014121181.

[51] B. Wang, et al., WNT1-inducible-signaling pathway protein 1 regulates the development of kidney fibrosis through the TGF-β1 pathway, Faseb. J. 34 (2020) 14507–14520, https://doi.org/10.1096/fj.202000953R.

[52] M. Agrawal, R. Swartz, Acute renal failure, Am. Fam. Physician 61 (2000) 2077–2088.

[53] D. Patschan, S. Patschan, G.A. Müller, Inflammation and microvasculopathy in renal ischemia reperfusion injury, J. Transplant. 2012 (2012), 764154, https://doi.org/10.1155/2012/764154.

[54] A. Shah, et al., Thioredoxin-interacting protein deficiency protects against diabetic nephropathy, J. Am. Soc. Nephrol. 26 (2015) 2963–2977, https://doi.org/10.1681/asn.2014050528.

[55] M.Z. Zhang, et al., Lysophosphatidic acid receptor antagonism protects against diabetic nephropathy in a type 2 diabetic model, J. Am. Soc. Nephrol. 28 (2017) 3300–3311, https://doi.org/10.1681/asn.2017010107.

[56] G. Igarashi, K. Iino, H. Watanabe, H. Ito, Remote ischemic pre-conditioning alleviates contrast-induced acute kidney injury in patients with moderate chronic kidney disease, Circ. J. 77 (2013) 3037–3044, https://doi.org/10.1253/circj.cj-13-0171.

[57] M. Bilban, et al., Carbon monoxide orchestrates a protective response through PPARgamma, Immunity 24 (2006) 601–610, https://doi.org/10.1016/j.immuni.2006.03.012.

[58] M. Nezu, et al., Transcription factor Nrf2 hyperactivation in early-phase renal ischemia-reperfusion injury prevents tubular damage progression, Kidney Int. 91 (2017) 387–401, https://doi.org/10.1016/j.kint.2016.08.023.

[59] E. Ku, et al., Associations between weight loss, kidney function decline, and risk of ESRD in the chronic kidney disease in children (CKiD) cohort study, Am. J. Kidney Dis. 71 (2018) 648–656, https://doi.org/10.1053/j.ajkd.2017.08.013.

[60] V.H. Haase, Hypoxia-inducible factor signaling in the development of kidney fibrosis, Fibrogenesis Tissue Repair 5 (2012) S16, https://doi.org/10.1186/1755-1536-5-S1-S16.

[61] A. Nabokov, R. Waldherr, E. Ritz, Demonstration of the proliferation marker Ki-67 in renal biopsies: correlation to clinical findings, Am. J. Kidney Dis. 30 (1997) 87–97, https://doi.org/10.1016/s0272-6386(97)90569-2.

[62] H.H. Chen, et al., Heme oxygenase-1 ameliorates kidney ischemia-reperfusion injury in mice through extracellular signal-regulated kinase 1/2-enhanced tubular epithelium proliferation, Biochim. Biophys. Acta 1852 (2015) 2195–2201, https://doi.org/10.1016/j.bbadis.2015.07.018.

[63] J. Matsumi, et al., Heme breakdown and ischemia/reperfusion injury in grafted liver during living donor liver transplantation, Int. J. Mol. Med. 29 (2012) 135–140, https://doi.org/10.3892/ijmm.2011.821.

[64] Z. Yuan, X. Yang, B. Wang, Redox and catalase-like activities of four widely used carbon monoxide releasing molecules (CO-RMs), Chem. Sci. 12 (2021) 13013–13020, https://doi.org/10.1039/d1sc03832j.

[65] H. Liu, et al., Inhibition of Brd4 alleviates renal ischemia/reperfusion injury-induced apoptosis and endoplasmic reticulum stress by blocking FoxO4-mediated oxidative stress, Redox Biol. 24 (2019), 101195, https://doi.org/10.1016/j.redox.2019.101195.

[66] K. Taguchi, et al., Biomimetic carbon monoxide delivery based on hemoglobin vesicles ameliorates acute pancreatitis in mice via the regulation of macrophage and neutrophil activity, Drug Deliv. 25 (2018) 1266–1274, https://doi.org/10.1080/10717544.2018.1477860.

[67] H.M. Southam, et al., Carbon-monoxide-releasing molecule-2 (CORM-2)' is a misnomer: ruthenium toxicity, not CO release, accounts for its antimicrobial effects, Antioxidants 10 (2021), https://doi.org/10.3390/antiox10060915.

[68] N.K. Campbell, H.K. Fitzgerald, A. Dunne, Regulation of inflammation by the antioxidant haem oxygenase 1, Nat. Rev. Immunol. 21 (2021) 411–425, https://doi.org/10.1038/s41577-020-00491-x.

[69] T. Suzuki, et al., Mitochonic acid 5 binds mitochondria and ameliorates renal tubular and cardiac myocyte damage, J. Am. Soc. Nephrol. 27 (2016) 1925–1932, https://doi.org/10.1681/asn.2015060623.

[70] R. Rodríguez-Romo, et al., AT1 receptor antagonism before ischemia prevents the transition of acute kidney injury to chronic kidney disease, Kidney Int. 89 (2016) 363–373, https://doi.org/10.1038/ki.2015.320.

[71] G. Yellen, Fueling thought: management of glycolysis and oxidative phosphorylation in neuronal metabolism, J. Cell Biol. 217 (2018) 2235–2246, https://doi.org/10.1083/jcb.201803152.

[72] L. Yu, et al., Modeling the genetic regulation of cancer metabolism: interplay between glycolysis and oxidative phosphorylation, Cancer Res. 77 (2017) 1564–1574, https://doi.org/10.1158/0008-5472.can-16-2074.

[73] P. Kaczara, et al., Carbon monoxide shifts energetic metabolism from glycolysis to oxidative phosphorylation in endothelial cells, FEBS Lett. 590 (2016) 3469–3480, https://doi.org/10.1002/1873-3468.12434.

[74] S. Lee, S.P. Hallis, K.A. Jung, D. Ryu, M.K. Kwak, Impairment of HIF-1α-mediated metabolic adaption by NRF2-silencing in breast cancer cells, Redox Biol. 24 (2019), 101210, https://doi.org/10.1016/j.redox.2019.101210.

[75] M. Correa-Costa, et al., Carbon monoxide protects the kidney through the central circadian clock and CD39, Proc. Natl. Acad. Sci. U. S. A. 115 (2018) E2302–E2310, https://doi.org/10.1073/pnas.1716747115.

[76] B. Plitzko, S. Loesgen, Measurement of oxygen consumption rate (OCR) and extracellular acidification rate (ECAR) in culture cells for assessment of the energy metabolism, Bio Protoc. 8 (2018), e2850, https://doi.org/10.21769/BioProtoc.2850.

[77] Z. Wang, et al., Silencing of hypoxia-inducible factor-1α gene attenuates chronic ischemic renal injury in two-kidney, one-clip rats, Am. J. Physiol. Ren. Physiol. 306 (2014) F1236–F1242, https://doi.org/10.1152/ajprenal.00673.2013.

[78] L. Li, et al., FoxO3 activation in hypoxic tubules prevents chronic kidney disease, J. Clin. Invest. 129 (2019) 2374–2389, https://doi.org/10.1172/jci122256.

[79] M.A. Gentile, Inhaled medical gases: more to breathe than oxygen, Respir. Care 56 (2011) 1341–1357, https://doi.org/10.4187/respcare.01442, discussion 1357-1349.

[80] G. Faleo, et al., Carbon monoxide ameliorates renal cold ischemia-reperfusion injury with an upregulation of vascular endothelial growth factor by activation of hypoxia-inducible factor, Transplantation 85 (2008) 1833–1840, https://doi.org/10.1097/TP.0b013e31817c6f63.

[81] J.L. Thomas, et al., Hypoxia-inducible factor-1α activation improves renal oxygenation and mitochondrial function in early chronic kidney disease, Am. J. Physiol. Ren. Physiol. 313 (2017) F282–F290, https://doi.org/10.1152/ajprenal.00579.2016.

[82] J.V. Tobin, et al., Pharmacological characterization of IW-1973, a novel soluble guanylate cyclase stimulator with extensive tissue distribution, antihypertensive, anti-inflammatory, and antifibrotic effects in preclinical models of disease, J. Pharmacol. Exp. Therapeut. 365 (2018) 664–675, https://doi.org/10.1124/jpet.117.247429.

[83] M. Buler, S.M. Aatsinki, V. Izzi, J. Hakkola, Metformin reduces hepatic expression of SIRT3, the mitochondrial deacetylase controlling energy metabolism, PLoS One 7 (2012), e49863, https://doi.org/10.1371/journal.pone.0049863.

[84] J. Park, Y. Joe, S.W. Ryter, Y.J. Surh, H.T. Chung, Similarities and distinctions in the effects of metformin and carbon monoxide in immunometabolism, Mol. Cell. 42 (2019) 292–300, https://doi.org/10.14348/molcells.2019.0016.

[85] J.R. Alonso, F. Cardellach, S. López, J. Casademont, O. Miró, Carbon monoxide specifically inhibits cytochrome c oxidase of human mitochondrial respiratory chain, Pharmacol. Toxicol. 93 (2003) 142–146, https://doi.org/10.1034/j.1600-0773.2003.930306.x.

[86] S. Cho, et al., NADPH oxidase 4 mediates TGF-β1/Smad signaling pathway induced acute kidney injury in hypoxia, PLoS One 14 (2019), e0219483, https://doi.org/10.1371/journal.pone.0219483.

[87] K. Richter, T. Kietzmann, Reactive oxygen species and fibrosis: further evidence of a significant liaison, Cell Tissue Res. 365 (2016) 591–605, https://doi.org/10.1007/s00441-016-2445-3.

[88] M.B. Hovater, W.Z. Ying, A. Agarwal, P.W. Sanders, Nitric oxide and carbon monoxide antagonize TGF-β through ligand-independent internalization of TβR1/ALK5, Am. J. Physiol. Ren. Physiol. 307 (2014) F727–F735, https://doi.org/10.1152/ajprenal.00353.2014.

[89] N. Jiang, et al., HIF-1α ameliorates tubular injury in diabetic nephropathy via HO-1-mediated control of mitochondrial dynamics, Cell Prolif 53 (2020), e12909, https://doi.org/10.1111/cpr.12909.

[90] A. Haschemi, et al., Carbon monoxide induced PPARγ SUMOylation and UCP2 block inflammatory gene expression in macrophages, PLoS One 6 (2011), e26376, https://doi.org/10.1371/journal.pone.0026376.

[91] I.T. Nizamutdinova, et al., Carbon monoxide (from CORM-2) inhibits high glucose-induced ICAM-1 expression via AMP-activated protein kinase and PPAR-gamma activations in endothelial cells, Atherosclerosis 207 (2009) 405–411, https://doi.org/10.1016/j.atherosclerosis.2009.05.008.

[92] K. Nakahira, et al., Carbon monoxide differentially inhibits TLR signaling pathways by regulating ROS-induced trafficking of TLRs to lipid rafts, J. Exp. Med. 203 (2006) 2377–2389, https://doi.org/10.1084/jem.20060845.

[93] J.T. Norman, I.M. Clark, P.L. Garcia, Hypoxia promotes fibrogenesis in human renal fibroblasts, Kidney Int. 58 (2000) 2351–2366, https://doi.org/10.1046/j.1523-1755.2000.00419.x.

[94] C.C. Yang, et al., Induction of HO-1 by 5, 8-dihydroxy-4',7-dimethoxyflavone via activation of ROS/p38 MAPK/Nrf2 attenuates thrombin-induced connective tissue growth factor expression in human cardiac fibroblasts, Oxid. Med. Cell. Longev. 2020 (2020), 1080168, https://doi.org/10.1155/2020/1080168.

[95] A. Weidemann, et al., HIF activation protects from acute kidney injury, J. Am. Soc. Nephrol. 19 (2008) 486–494, https://doi.org/10.1681/asn.2007040419.

[96] P. Singh, S.E. Ricksten, G. Bragadottir, B. Redfors, L. Nordquist, Renal oxygenation and haemodynamics in acute kidney injury and chronic kidney disease, Clin. Exp. Pharmacol. Physiol. 40 (2013) 138–147, https://doi.org/10.1111/1440-1681.12036.

[97] C.P.C. Ow, M.M. Ullah, J.P. Ngo, A. Sayakkarage, R.G. Evans, Detection of cellular hypoxia by pimonidazole adduct immunohistochemistry in kidney disease: methodological pitfalls and their solution, Am. J. Physiol. Ren. Physiol. 317 (2019) F322–f332, https://doi.org/10.1152/ajprenal.00219.2019.

[98] H. Saito, et al., Hepatic sulfotransferase as a nephropreventing target by suppression of the uremic toxin indoxyl sulfate accumulation in ischemic acute kidney injury, Toxicol. Sci. 141 (2014) 206–217, https://doi.org/10.1093/toxsci/kfu119.

[99] T. Vera, J.R. Henegar, H.A. Drummond, J.M. Rimoldi, D.E. Stec, Protective effect of carbon monoxide-releasing compounds in ischemia-induced acute renal failure, J. Am. Soc. Nephrol. 16 (2005) 950–958, https://doi.org/10.1681/asn.2004090736.

[100] N.I. Skrypnyk, L.J. Siskind, S. Faubel, M.P. de Caestecker, Bridging translation for acute kidney injury with better preclinical modeling of human disease, Am. J. Physiol. Ren. Physiol. 310 (2016) F972–F984, https://doi.org/10.1152/ajprenal.00552.2015.
[101] E.A. Hoste, et al., The epidemiology of cardiac surgery-associated acute kidney injury, Int. J. Artif. Organs 31 (2008) 158–165, https://doi.org/10.1177/039139880803100209.
[102] N. Perico, D. Cattaneo, M.H. Sayegh, G. Remuzzi, Delayed graft function in kidney transplantation, Lancet 364 (2004) 1814–1827, https://doi.org/10.1016/s0140-6736(04)17406-0.
[103] A. Nakao, et al., Application of carbon monoxide for treatment of acute kidney injury, Acute Med. Surg. 1 (2014) 127–134, https://doi.org/10.1002/ams2.38.
[104] J. Yoshida, et al., Ex vivo application of carbon monoxide in UW solution prevents transplant-induced renal ischemia/reperfusion injury in pigs, Am. J. Transplant. 10 (2010) 763–772, https://doi.org/10.1111/j.1600-6143.2010.03040.x.
[105] A. Nakao, et al., Low-dose carbon monoxide inhibits progressive chronic allograft nephropathy and restores renal allograft function, Am. J. Physiol. Ren. Physiol. 297 (2009) F19–F26, https://doi.org/10.1152/ajprenal.90728.2008.
[106] A. Nakao, et al., Ex vivo carbon monoxide prevents cytochrome P450 degradation and ischemia/reperfusion injury of kidney grafts, Kidney Int. 74 (2008) 1009–1016, https://doi.org/10.1038/ki.2008.342.
[107] A.M. Foskett, et al., Phase-directed therapy: TSG-6 targeted to early inflammation improves bleomycin-injured lungs, Am. J. Physiol. Lung Cell Mol. Physiol. 306 (2014) L120–L131, https://doi.org/10.1152/ajplung.00240.2013.
[108] P. Sawle, et al., Carbon monoxide-releasing molecules (CO-RMs) attenuate the inflammatory response elicited by lipopolysaccharide in RAW264.7 murine macrophages, Br. J. Pharmacol. 145 (2005) 800–810, https://doi.org/10.1038/sj.bjp.0706241.
[109] H. Maeda, et al., Repeated administration of Kupffer cells-targeting nanoantioxidant ameliorates liver fibrosis in an experimental mouse model, Biol. Pharm. Bull. 43 (2020) 93–101, https://doi.org/10.1248/bpb.b19-00599.
[110] D. Wen, et al., Inhibitor of DNA binding 1 is induced during kidney ischemia-reperfusion and is critical for the induction of hypoxia-inducible factor-1α, BioMed Res. Int. 2016 (2016), 4634386 https://doi.org/10.1155/2016/4634386.